

# Neutron Diffraction and Optics of a Noncentrosymmetric Crystal. New Feasibility of a Search for Neutron EDM

V.V. Fedorov, V.V. Voronin\*

October 4, 2018

## Abstract

Recently strong electric fields (up to  $10^9$  V/cm) have been discovered, which affect the neutrons moving in noncentrosymmetric crystals. Such fields allow new polarization phenomena in neutron diffraction and optics and provide, for instance, a new feasibility of a search for the neutron electric dipole moment (EDM). A strong interplanar electric field of the crystal and a sufficiently long time for the neutron passage through the crystal for Bragg angle close to  $\pi/2$  in the case of Laue diffraction make it possible to reach the sensitivity achieved with the most sensitive now magnetic resonance method using ultra cold neutrons (UCN method).

A series of experiments was carried out in a few last years on study of the dynamical diffraction of polarized neutrons in thick (1–10 cm) quartz crystals, using the forward diffraction beam and Bragg angles close to  $90^\circ$ . As well new neutron optics phenomena were investigated. The following effects was first observed:

- the effect of an essential time delay of a diffracting neutron inside the crystal for Bragg angles close to  $\pi/2$ ;
- the phenomenon of a neutron beam depolarization in time of Laue diffraction by noncentrosymmetric  $\alpha$ -quartz crystal;
- the effect of a neutron-optical spin rotation for neutrons moving through a noncentrosymmetric crystal with the energies and directions far from the Bragg ones;
- the controlled spin rotation effect for the Bragg reflected (from a small part of crystal near its exit face) neutrons in a slightly deformed quartz crystal.

The feasibility of experiment on a search for neutron EDM using Laue diffraction in crystals without a center of symmetry was tested at the reactors: WWR-M in Gatchina and HFR in Grenoble. It was shown that the sensitivity can reach  $(3 - 6) \cdot 10^{-25}$  e · cm per day for the available quartz crystal and cold neutron beam flux.

## 1 Introduction

The origin of CP-symmetry violation (where C is a charge conjugation and P is a spatial inversion) is of a great interest since its discovery in the decay of neutral K-mesons about 40 years ago. CP violation leads in turn to the violation of the time reversal symmetry (T)

---

\*Petersburg Nuclear Physics Institute, 188300, Gatchina, St.Petersburg, Russia, E-mail: vvv@mail.pnpi.spb.ru. This work is a basis for Dr. of Sci. thesis of V.V.Voronin

through the CPT invariance (CPT-theorem). Existence of nonzero neutron EDM requires violation of both P and T invariance. Different theories of CP violation give widely varying predictions for a neutron EDM (see for instance [1, 2]). Therefore, the new experimental limits on the EDM value would be of great importance for understanding the nature of the CP violation as well as of the Universe baryon asymmetry, which are beyond the Standard Model.

The most precision method of the EDM measurement now is the magnetic resonance one [3, 4, 5]<sup>1</sup> using the ultracold neutrons (UCN method).

Here we shall discuss another possible way for the neutron EDM search, using Laue diffraction of the cold neutrons in the noncentrosymmetric crystal [6]. Earlier [7] we have shown that the neutron, moving through a noncentrosymmetric crystal, may be influenced with a strong interplanar electric field. Its value depends on direction and value of a neutron wave vector, reaching a maximum (up to  $10^9$  V/cm), when the Bragg condition for some system of crystallographic planes is satisfied. These fields result in new polarization phenomena observable in neutron diffraction and optics. In particular, the Schwinger interaction of the neutron magnetic moment with such fields leads to spin dependence of the neutron Pendellösung picture [7]. The Pendellösung phase shift accompanying the spin flip was measured first in ref. [7], and so the interplanar electric field was determined in the experiment on dynamical Laue diffraction of polarized neutrons for the (110)-plane of the  $\alpha$ -quartz crystal. Experimental value of the field was obtained to be equal  $E_{(110)} = (2.10 \pm 0.12) \times 10^8$  V/cm and had coincided with the theoretical one.

The interplanar electric fields are more than four orders of magnitude higher than those used in the UCN methods [3, 4, 5] of the neutron EDM search. So it was a natural idea [8, 9, 10] (arisen anew after Shull and Nathans [11]) to use these crystal fields for searching the neutron EDM (see also [12, 13]). However, the value of the crystal field turned out to be still insufficient to reach the sensitivity of the UCN method, but it was shown [8] that use of Laue diffraction for EDM measurements with the Bragg angles close to  $90^\circ$  would essentially increase the time, the neutron spends in crystal under the strong electric field.

Two variants of the method, using the Laue diffraction of polarized neutrons in the crystals without a centre of symmetry, were proposed for this purpose. One of them is the double crystal variant [8] based on a spin dependence of the Pendellösung picture phase and the second is the polarization method [9] using the depolarization effect for neutrons diffracting in the noncentrosymmetric crystals. It was shown [8, 9] that the sensitivity of the method to measure the neutron EDM may be increased more than by an order of magnitude by a choice of Bragg angles close to  $\pi/2$ , so it may exceed (with the higher luminosity taken into account) the sensitivity of the UCN method [3, 4, 5]. That is possible for Laue diffraction scheme only. But only the experimental study of these effects can answer the question on actual sensitivity of the method to measure the neutron EDM.

A hypothetical idea to use the interplanar electric fields (if they did exist) for the neutron EDM search was discussed in the review [13]. But such crystal properties were not known at that time.

The importance to consider the crystal noncentrosymmetry was previously pointed out in ref. [14]. Authors [14] were the first who paid attention to an existence of the

---

<sup>1</sup>Last experimental result for a neutron EDM obtained by this method is  $d_n \leq 6.3 \cdot 10^{-26}$  e-cm at the 90% confidence level [5].

interference between the electric and nuclear structure amplitudes for neutrons diffracted by noncentrosymmetric crystal and proposed to study the Schwinger interaction using such crystals.

In the work [10] the effect of neutron spin rotation due to such interference has been discussed. Similar, but more detailed theory of neutron optical activity and dichroism for diffraction in noncentrosymmetric crystals has been developed in ref. [12].

It has been shown [10] that the spin rotation effect in a non-absorbing crystal can take place only for Bragg scheme of diffraction. The deviation from the Bragg condition by about the Bragg width is necessary in this case to observe the effect for the transmitted beam. That reduces the effect, because it is proportional to  $1/\sqrt{1+w^2}$ , where  $w$  is the parameter of angular deviation (measured in the units of Bragg halfwidth) from the Bragg direction, see [8]. The nuclear absorption is necessary to have a spin rotation effect in the case of Laue diffraction [10, 12].

The possibility of a search for neutron EDM by measuring a spin rotation angle was analyzed for the Bragg diffraction scheme [10] and for the Laue scheme [12].

We have shown [7] that for some system of crystallographic planes in noncentrosymmetric crystals the positions of the electric potential maxima can be shifted relative to those of a nuclear potential. Hence, the diffracted neutrons will move in the crystal under a strong ( $10^8 - 10^9$  V/cm) interplanar electric field (because of the neutron concentration on the nuclear potential maxima or between them). Such a concept turned out to be very fruitful for further consideration and understanding the different phenomena, concerning the neutron diffraction and the optics in noncentrosymmetric crystals [7, 8]. For example it allowed to predict and to give a simple description of such new effects as the spin dependence of the pendulum phase, the depolarization of the diffracting neutron beams, the independence of the effects due to the Schwinger interaction on the neutron wavelength and Bragg angle for given crystallographic planes etc. [9, 15, 16].

We should note also, that the Bragg reflection of neutrons from the neutron-absorbing centrosymmetric crystal of CdS was used earlier [11] for EDM search. But the sensitivity of this method is much lower than that of UCN-method, because the depth of neutron penetration into the crystal, which determines a time the neutron stay in crystal, was very small (about  $7 \cdot 10^{-2}$  cm). Now a new variant of the method is proposed and developed, using the multiple reflections from the silicon centrosymmetric crystal [17, 18].

In the work [19] it was reported that the effect of the neutron spin rotation has been observed due to the spin-orbit (Schwinger) interaction, using the Bragg scheme of the diffraction in the noncentrosymmetric crystal with a small deviation of a neutron momentum direction (by about a few Bragg width) from the Bragg one, because the effect disappears for the exact Bragg direction in this case. However, the experimental value of the spin rotation angle [19] turned out to be a few times less than the theoretical one. Authors were in difficulty to explain the origin of such discrepancy, but it was very likely due to imperfection of the used crystal.

Here we consider neutron-optic effects for neutrons, moving through a noncentrosymmetric crystal with the energies and the directions far from the Bragg ones, when the deviation from the exact Bragg condition reaches ( $10^3 - 10^5$ ) Bragg widths.

The theoretical estimations have shown [20], that for the polar noncentrosymmetric crystal ( $PbTiO_3$ , for instance) the value of a resultant electric field, acting on a neutron, can reach  $\approx 2 \times 10^6$  V/cm for wide range (about four orders exceeding the Bragg width)

of the neutron directions and wavelengths. Such a field is a result of superposition of the fields from a few different crystallographic planes. Therefore, the spin rotation effects may be not too small in neutron optics in comparison with the diffraction case.

The observation of such effects may be of interest for development of new methods for searching the neutron EDM. It also may be useful for experimental searching the T-odd part of the nuclear interaction, using neutrons with energy close to the P-resonance one [21], because it is hardly possible to observe dynamical diffraction in a large crystal for neutrons with the energy  $\sim 1$  eV because of too high requirements to a crystal quality.

The phenomenon can be used also for measurements of the interplanar electric fields affecting the neutrons in the crystals without centre of symmetry. A new specific spin neutronography arises in this case for crystallographic planes with nonzero electric fields.

## 2 Diffraction in a noncentrosymmetric crystal

As it follows from the dynamical diffraction theory, a movement of a neutron through the crystal in a direction close to the Bragg one for some system of crystallographic planes can be described by two kinds of Bloch waves  $\psi^{(1)}$  and  $\psi^{(2)}$  (see for example, [22]), formed as a result of neutron interaction with the periodic nuclear potential [8]  $V_g^N(\mathbf{r}) = V_0^N + 2v_g^N \cos(\mathbf{g}\mathbf{r})$ , where  $\mathbf{g}$  is a reciprocal lattice vector describing the system of crystallographic planes,  $|\mathbf{g}| = 2\pi/d$ ,  $d$  is an interplanar spacing,  $V_0^N$  is the average nuclear potential of the crystal,

$$\psi^{(1)} = \cos \gamma e^{i\mathbf{k}^{(1)}\mathbf{r}} + \sin \gamma e^{i\mathbf{k}_g^{(1)}\mathbf{r}}, \quad (1)$$

$$\psi^{(2)} = -\sin \gamma e^{i\mathbf{k}^{(2)}\mathbf{r}} + \cos \gamma e^{i\mathbf{k}_g^{(2)}\mathbf{r}}, \quad (2)$$

where  $\text{tg } 2\gamma = |U_g|/\Delta \equiv 1/w = \gamma_B/\Omega$ ;  $0 < \gamma < \pi/2$ ,  $U_g^N = 2mv_g^N/\hbar^2$ ,  $\mathbf{k}_g^{(1,2)} = \mathbf{k}^{(1,2)} + \mathbf{g}$ ;  $\Delta = (k_g^2 - k^2)/2$ . The parameter  $w$  is the ratio of angular deviation from the exact Bragg direction  $\Omega = \theta - \theta_B$  to the angular Bragg width  $\gamma_B$ , therefore  $w$  describes the relative deviation from the exact Bragg condition.

The intensities of direct and reflected waves in the states (1), (2) are given by

$$\cos^2 \gamma = \frac{1}{2} \left[ 1 + \frac{\Delta_g}{\sqrt{\Delta_g^2 + |U_g|^2}} \right] = \frac{1}{2} \left[ 1 + \frac{w}{\sqrt{1 + w^2}} \right].$$

The expressions (1), (2) describe two standing waves (in the direction  $\mathbf{g}$  normal to the crystallographic planes), which are moving in the direction  $\mathbf{k}_{\parallel}^{(1,2)} = \mathbf{k}^{(1,2)} + \mathbf{g}/2$  along the planes (see Fig. 1). A small difference of the wave vectors  $k^{(1)}$ ,  $k^{(2)}$  is a result of neutron concentration on "nuclear" planes (for  $\psi^{(1)}$ ) and between them (for  $\psi^{(2)}$ ),

$$k^{(1,2)2} = K^2 - \Delta \pm \sqrt{\Delta^2 + |U_g|^2}. \quad (3)$$

where  $K^2 = k_0^2 + U_0^N \equiv 2m(E + V_0^N)/\hbar^2$ ,  $m$ ,  $E$ ,  $k_0$  are respectively the mass, energy and wave vector of the incident neutron.

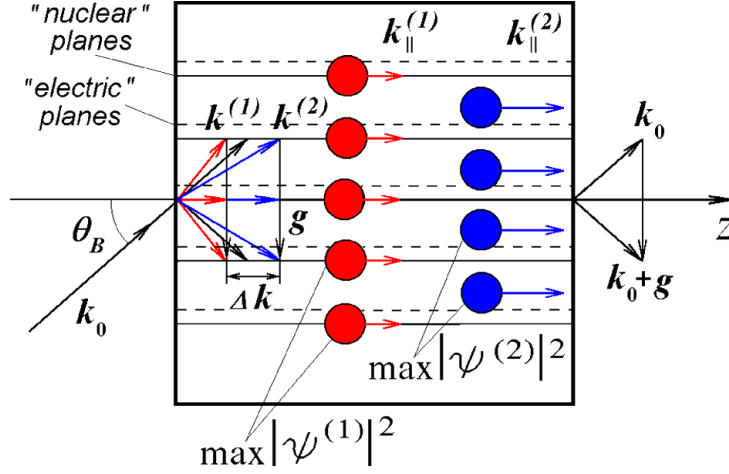


Figure 1: Passage neutron through the crystal.

The values  $V_0^N$ ,  $v_g^N$  have an order of  $10^{-7}$  eV, so for thermal and cold neutrons with the energies of  $(10^{-1} - 10^{-3})$  eV we can consider that  $k^{(1)} \approx k^{(2)} \approx k$ . The propagation velocities of these waves along the crystallographic planes are<sup>2</sup>

$$v_{\parallel}^{(1,2)} = \frac{\hbar}{m} |\mathbf{k}^{(1,2)} + \mathbf{g}/2| = \frac{\hbar}{m} k^{(1,2)} \cos \theta_B \approx v \cos \theta_B, \quad (4)$$

where  $v = \hbar k/m = 2\pi\hbar/(\lambda m) = \pi\hbar/(md \sin \theta_B)$  is the velocity of the incident neutron,  $\theta_B$  is the Bragg angle,  $\lambda = 2\pi/k$  is the wavelength of the incident neutron ( $\lambda = 2d \sin \theta_B$ ). A number of the dynamical diffraction phenomena (see, for example, [22, 23, 24]), including effects caused by the neutron EDM [8, 9], are determined not by a total neutron velocity  $v$ , but its component along the crystallographic planes  $v_{\parallel} = v \cos \theta_B$ . In particular, the time the diffracting neutron spends in crystal, which equal to  $\tau_L = L/(v \cos \theta_B) \approx L/[v(\pi/2 - \theta_B)]$ , sharply grows for Bragg angles close to  $\pi/2$ , where  $L$  is the thickness of a crystal. That allows to increase the sensitivity of the diffraction method to neutron EDM at least by an order [8, 9]. Therefore the values<sup>3</sup>  $E\tau$  can be of the same order for UCN and diffraction method (for Bragg angles sufficiently close to  $\pi/2$ ) [8, 9] despite the fact that the storage time for UCN ( $\sim 100$  s [3]) is essentially more than the time of a neutron passage through the crystal<sup>4</sup>.

We proposed the polarization method for searching a neutron EDM based on the predicted effect of depolarization of the diffracted neutron beam [9] in noncentrosymmetric crystal. This method has some advantages (such as its relative simplicity and less sensitivity to crystal imperfection) over the method based on the spin dependence of the neutron

<sup>2</sup>Here we neglect the Pendellösung oscillations (arising from the interference of waves of different type) because in our case they are averaged over Bragg angles for a slightly divergent beam.

<sup>3</sup>The set-up sensitivity is determined by  $\sigma(D) \propto 1/E\tau\sqrt{N}$ , where  $\sigma(D)$  is an absolute error of EDM measurement,  $N$  is a total value of accumulated events.

<sup>4</sup>The ways of possible improving the UCN-method are discussed [25].

Pendellösung phase [8].

Essence of the effect is as follows. In the noncentrosymmetric crystal the diffracting neutrons in two Bloch states are moving under opposite electric fields [7, 8, 15] because of the shift of the "electric" planes relative to the "nuclear" ones, see Fig. 1. We mean that "nuclear" or "electric" planes are determined by the maximum positions of the corresponding periodic potentials of this plane system

$$V_g^N(\mathbf{r}) = V_0^N + 2v_g^N \cos(\mathbf{g}\mathbf{r}),$$

$$V_g^E(\mathbf{r}) = V_0^E + 2v_g^E \cos(\mathbf{g}\mathbf{r} + \phi_g^E),$$

the shift  $\phi_g^E$  may be calculated using the crystal structure. The electric field of the plane system has a form

$$\mathbf{E}(\mathbf{r}) = -\text{grad } V_g^E(\mathbf{r}) = 2v_g^E \mathbf{g} \sin(\mathbf{g}\mathbf{r} + \phi_g^E).$$

So the mean electric fields acting on a neutron in the states  $\psi^{(1)}$  and  $\psi^{(2)}$  will be equal

$$\langle \psi^{(1)} | \mathbf{E}(\mathbf{r}) | \psi^{(1)} \rangle = -\langle \psi^{(2)} | \mathbf{E}(\mathbf{r}) | \psi^{(2)} \rangle = \frac{\mathbf{E}_g}{\sqrt{1+w^2}} = \frac{\mathbf{g}v_g^E \sin \phi_g^E}{\sqrt{1+w^2}}. \quad (5)$$

where

$$\mathbf{E}_g \equiv \mathbf{g}v_g^E \sin \phi_g^E, \quad (6)$$

is the maximum electric field acting on a neutron under the exact Bragg condition ( $w = 0$ ).

Therefore spins in these states will rotate in the opposite directions due to Schwinger interaction, that in turn will lead to a decrease of the neutron beam polarization (see Fig. 2). If an initial spin orientation is normal to the "Schwinger" magnetic field  $\mathbf{H}_g^S = [\mathbf{E}_g \times \mathbf{v}_\parallel]/c$ , then for the case  $w \ll 1$  (exact Bragg condition) the spin rotation angle in both states will be equal to [8, 15]

$$\Delta\phi_0^S = \pm \frac{2\mu H_g^S L}{\hbar v_\parallel} = \pm \mu_n \frac{eE_g L}{m_p c^2}, \quad (7)$$

because  $\mathbf{E}_g \perp \mathbf{v}_\parallel$  and  $H_g^S = E_g v_\parallel / c$ . Here the signs  $\pm$  are related to different states (1), (2) respectively,  $\mu_n = -1.9$  is the neutron magnetic moment in nuclear magnetons. As a result the value of neutron beam polarization  $P$  will depend on  $\Delta\phi_0^S$  in the following way<sup>5</sup>:

$$P = P_0 \cos \Delta\phi_0^S = P_0 \cos \left( \frac{\mu_n e E_g L}{m_p c^2} \right), \quad (8)$$

$P_0$  is the incident beam polarization (see Fig. 2).

The polarization  $P$  can be decreased down to zero by a choice of such a crystal thickness  $L_0$  that makes the spin rotation angles equal to  $\pm\pi/2$ . Theoretical calculation for (110)-planes of  $\alpha$ -quartz gives  $L_0 = 3.5$  cm.

The existence of the neutron EDM leads to a slight polarization  $P_{EDM}$  along  $\mathbf{H}_g^S$ , equal to

$$P_{EDM} = \frac{4DE_g L_0}{\pi \hbar v_\parallel} = \frac{4D}{\pi \mu} \cdot \frac{c}{v \cos \theta_B} \propto \frac{1}{\pi/2 - \theta_B}, \quad (9)$$

<sup>5</sup>This result is obtained averaging the Pendellösung oscillations over Bragg angles. The angular period of this oscillations in our case is  $\sim 10^{-5}$  rad and the angular divergence of the neutron beam is  $\sim 10^{-2}$  rad.

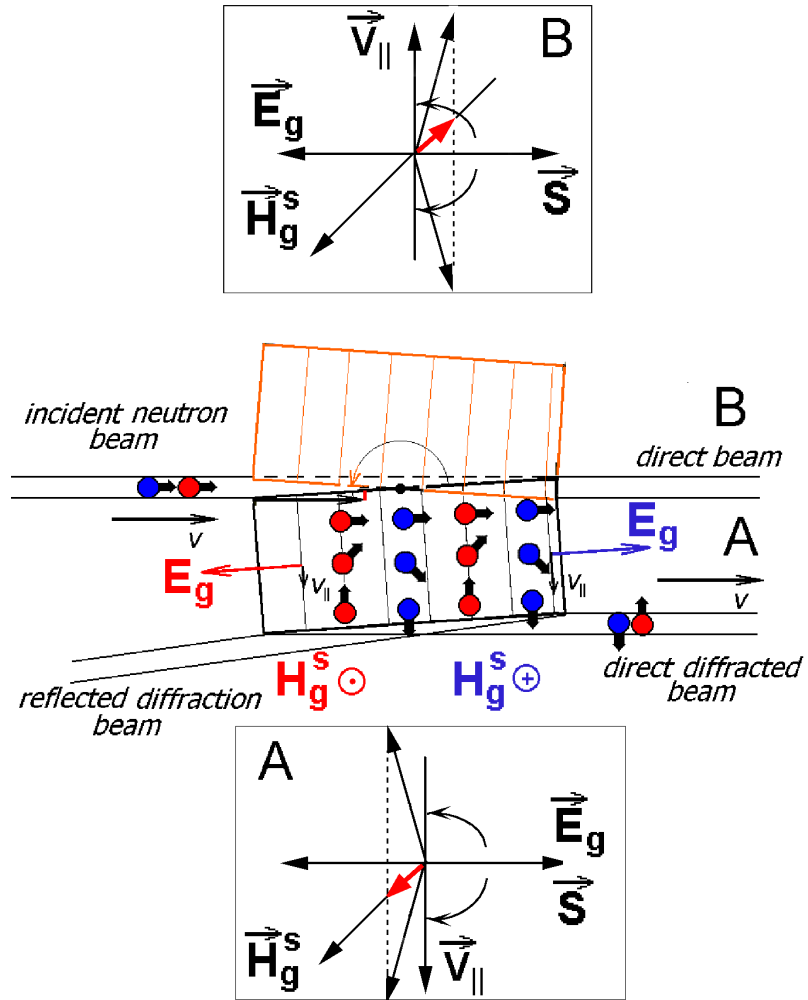


Figure 2: The neutron spin for two Bloch waves (shown schematically as the red and blue circles) will rotate in opposite direction under opposite fields. When the angles of spin rotation become equal to  $\pi/2$ , the both diffracted neutron beams will be depolarized entirely. The existence of neutron EDM will result in a polarization along the Schwinger magnetic field. The sign of this polarization will be different for two crystal position A and B.

because  $\cos\theta_B \propto \pi/2 - \theta_B$  for  $\theta_B \rightarrow \pi/2$ . Here  $D$  is the neutron EDM. The turn of the crystal by the angle  $2\theta_B$  (see Fig. 2) will change the  $P_{EDM}$  sign but will not do that for residual polarization. High precision of the crystal turning (better than  $10^{-5}$  rad) gives the possibility to exclude the systematic errors and to select the EDM effect.

The principal scheme of the Laue diffraction method to search for the neutron EDM [26, 27] is shown in Fig. 3. For two crystal positions R and L with the same Bragg angle but with opposite directions of the electric field, the polarization  $P_{EDM}$  will have opposite signs whereas a residual polarization will have the same sign for both crystal positions. Therefore we should put the initial neutron spin along the neutron velocity (Y axis) and compare the components of the polarization along the Z axis for two crystal position marked by R and L in Fig. 3.

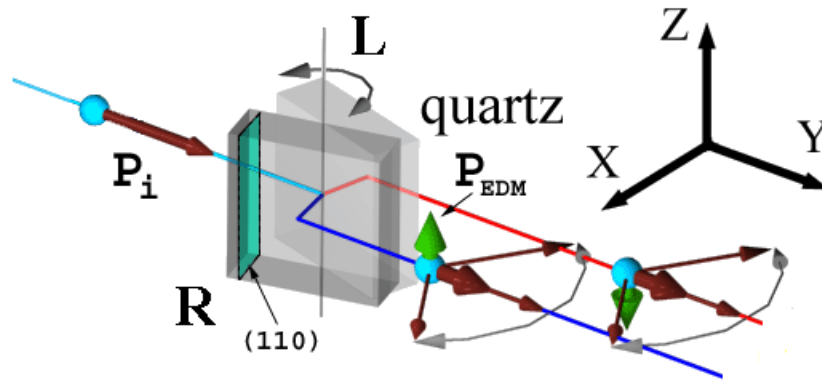


Figure 3: Scheme of the experiment for a neutron EDM search by Laue diffraction. The presence of a neutron EDM will lead to a small Y-component of the polarization, which will have different signs for the two crystal positions R and L.

As it follows from (7) the effect due to the Schwinger interaction does not depend on such neutron properties as the energy, wavelength and the Bragg angle. It is determined by the property of crystal and by the fundamental constants only. For given crystal it is the same for any Bragg angles. That gives an additional way to eliminate a false effect concerned with the Schwinger interaction by carrying out the measurements for two Bragg angles, for example. The EDM effect (9) (in contrast to the Schwinger one) depends on the Bragg angle. It essentially increases for  $\theta_B \rightarrow \pi/2$ .

### 3 Measurement of time the neutron spends in crystal

Two experiments described below on observing the effect of the neutron time delay in the crystal and the depolarization effect were carried out at the WWR-M reactor in PNPI (Gatchina, Russia). The scheme of experimental setup is shown in Fig. 4<sup>a</sup>) [28, 29].

The neutron beam formed by neutron guides 1,2 is diffracted by the noncentrosymmetric  $\alpha$ -quartz crystal 6 (the reflecting (110) planes are normal to the large crystal surfaces) and



is registered by the detectors 11.

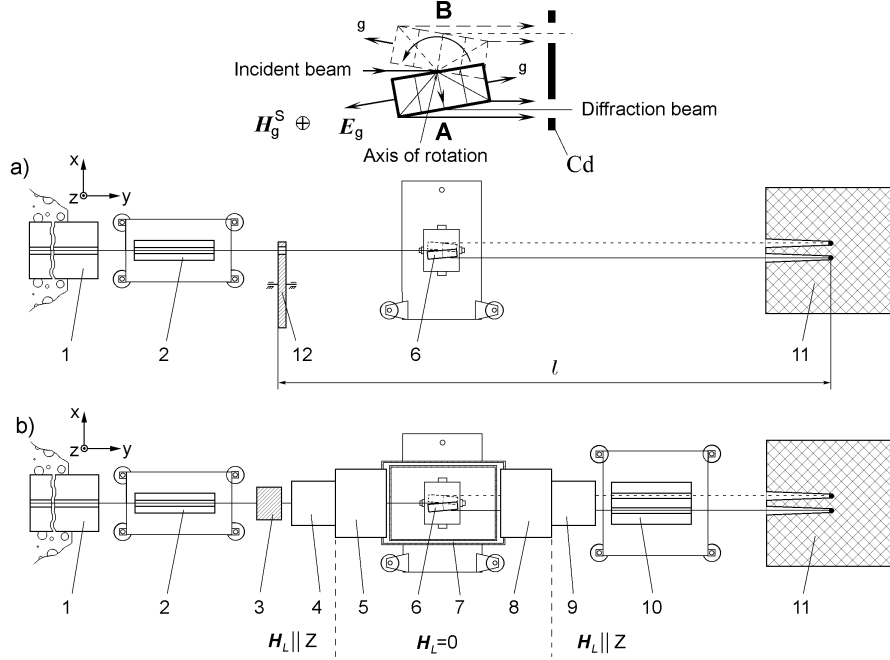


Figure 4: Two modifications of the experimental set-up: **a)** for time-of-flight measurements, **b)** for measurement of the depolarization effect. **1** is a reactor interchannel neutron guide, **2** is a multislit polarizing neutron guide, **3** is the  $BeO$  polycrystal filter (120 mm), **4,9** are spin-guide coils, **5,8** are spin-rotation coils, **6** is the  $\alpha$ -quartz single crystal, (sizes are  $14 \times 14 \times 3.5 \text{ cm}^3$ ), **10** is a double multislit polarizing neutron guide, **11** are neutron detectors, **12** is a beam chopper. **A** and **B** are two crystal positions with the same Bragg angles,  $\mathbf{g}$  is the reciprocal lattice vector for the (110)-plane,  $\mathbf{H}_L$  is the guiding magnetic field,  $l$  is the TOF length.

All neutrons diffracted by the different crystallographic plane systems (for which the Bragg conditions are satisfied) give the contribution to the intensity of the direct diffracted beam. We used the time-of-flight (TOF) technique to select the specified reflection. The mechanical beam chopper **12** was placed before the crystal. The typical TOF spectrum is shown in Fig. 5. The peaks corresponding to neutrons diffracted by the different crystallographic planes are clearly visible in the figure.

If the crystal is located between the beam chopper and the neutron detector, the total time of flight of neutron with the wavelength  $\lambda = 2d \sin \theta_B$  will be:

$$\tau_f = \tau_l + \tau_L = \frac{l}{v} + \frac{L}{v \cos \theta_B} = \frac{dm}{\hbar \pi} (l \sin \theta_B + L \text{tg} \theta_B), \quad (10)$$

where  $\tau_l$  is the neutron time of flight for a distance  $l$ ,  $\tau_L$  is the time a neutron spends in the crystal,  $L$  is the thickness of the crystal,  $\theta_B$  is the Bragg angle (for the (110) plane of

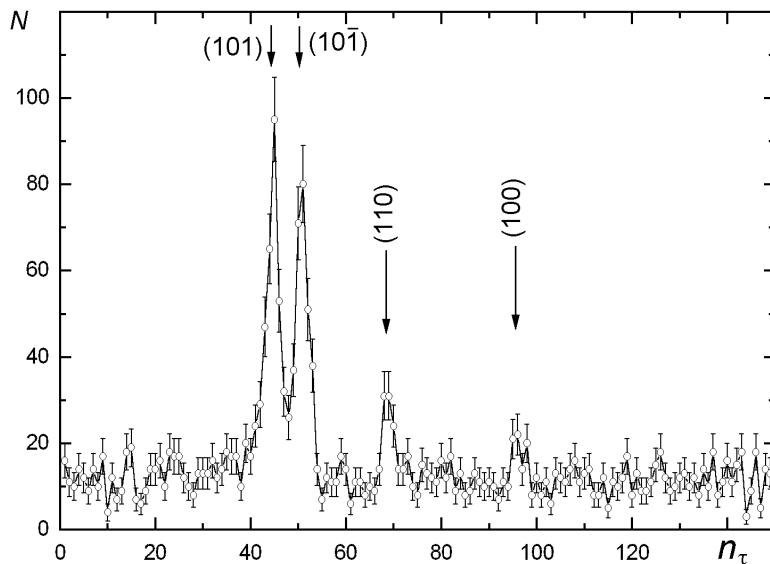


Figure 5: TOF spectrum of the forward diffracted neutrons for Bragg angle  $\theta_B = 75^\circ$ .  $n_\tau$  is the order number of the TOF channel. The width of the TOF channel is equal  $\simeq 51.2 \mu\text{s}$ .  $N$  is the number of accumulated events.

the  $\alpha$ -quartz crystal  $d = 2.4564\text{\AA}$ ). As follows from (10) the time  $\tau_L$  of a neutron delay in the crystal depends on the Bragg angle as  $\text{tg}\theta_B$ , while the  $\tau_l \propto \sin\theta_B$ , so  $\tau_L$  may give a very essential contribution to the total TOF of neutrons  $\tau_f$  for  $\theta_B$  close to  $\pi/2$ , because  $\tau_L/\tau_l \simeq L/[l(\pi/2 - \theta_B)]$ .

A dependence on the Bragg angle of the neutron TOF for forward beam diffracted by the (110)-plane is given in Fig. 6.

A solid curve describes the calculated dependence  $\tau_f(\theta_B)$  (see (10)), and the dotted curve does that for  $\tau_l(\theta_B)$ . One can see a good agreement between experimental (black points) and theoretical dependencies  $\tau_f(\theta_B)$ . A control experiment, when the chopper of a neutron beam was placed between the crystal and detector, was also carried out. In this case the delay of neutron in the crystal does not give a contribution to the measured value and the position of the line  $\tau_l(\theta_B)$  for (110)-reflection should coincide with the dotted curve. That is what we have observed experimentally (open points). On insertion in Fig. 6 the theoretical and experimental dependencies  $\tau_L(\theta_B)$  are shown.

So the experiment have proved that the time of neutron delay in the crystal is not determined by the total neutron velocity  $v$ , but its component  $v_{\parallel}$  along the crystallographic plane. In particular, for  $\theta_B = 87^\circ$  we find that  $\tau_L = (0.90 \pm 0.02)$  ms and  $v_{\parallel} = (39 \pm 1)$  m/s, while  $v = 808$  m/s.

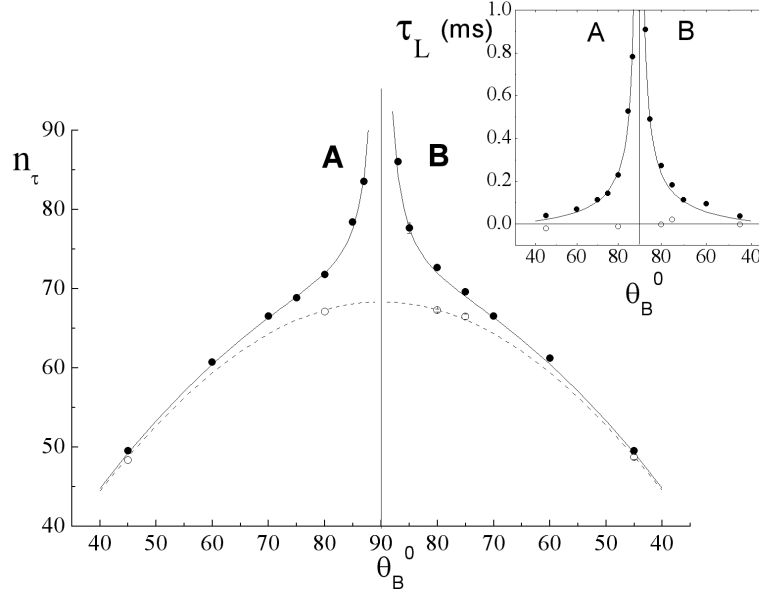


Figure 6: Dependence of the neutron TOF on the Bragg angle for forward diffracted beam.

## 4 Measurement of the depolarization effect

So we have shown that the polarization of the diffracted beams will be zero for crystal thickness  $L = 3.5$  cm, if the initial neutron polarization is perpendicular to the Schwinger magnetic field  $\mathbf{H}_g^S$ , while for initial polarization parallel to  $\mathbf{H}_g^S$  will stay completely polarized. We used a set of different angles between directions of initial neutron polarization and Schwinger magnetic field to study this effect in detail.

The scheme of the experimental setup is shown in Fig. 4<sup>b</sup>), see also [29, 30]. The polarization vector  $\mathbf{P}_0$  of a neutron after passage through the polarizing neutron guide 2 and the filter 3 is directed along  $\mathbf{H}_g^S$  by the coil 4, then it turns round by the angle  $\alpha$  by the coil 5. If the crystal does not influence the spin orientation, the polarization vector will be restored in the initial direction along the  $\mathbf{H}_g^S$  by the coil 8. The behavior of the neutron spin for the case of  $\alpha = 90^\circ$  is shown in Fig. 7. We use the same coordinate system  $(X, Y, Z)$  in Fig. 7 and Fig. 4.

The dependence of a neutron beam intensity on the angle  $\alpha$  after the analyzer 10 was studied to observe the depolarization effect for diffracted neutrons. The analyzer 10 transmits the neutrons with the polarization parallel to  $\mathbf{H}_g^S$  only. The measurements are similar to those, using a spin-echo technique.

The neutron beam passed through the polycrystalline BeO filter 3 of a 120 mm thickness to reduce the contribution of the background reflections (see Fig. 5) to the forward diffraction beam. The residual contribution of them was estimated to be  $\simeq (20 \pm 10)\%$  of the useful intensity of neutrons diffracted by the (110) plane. The uncertainty of this contribution results in a systematic error of a measured value.

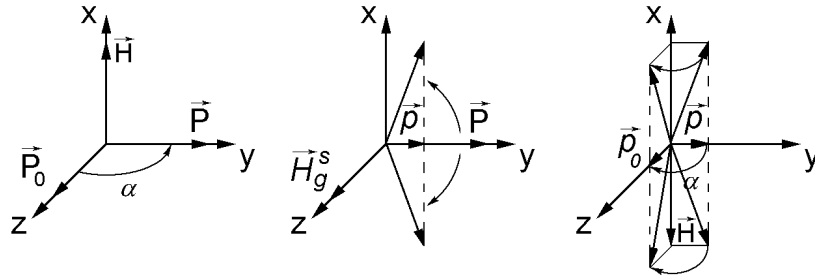


Figure 7: The behavior of the diffracted neutron spin for the case  $\alpha = 90^\circ$ .

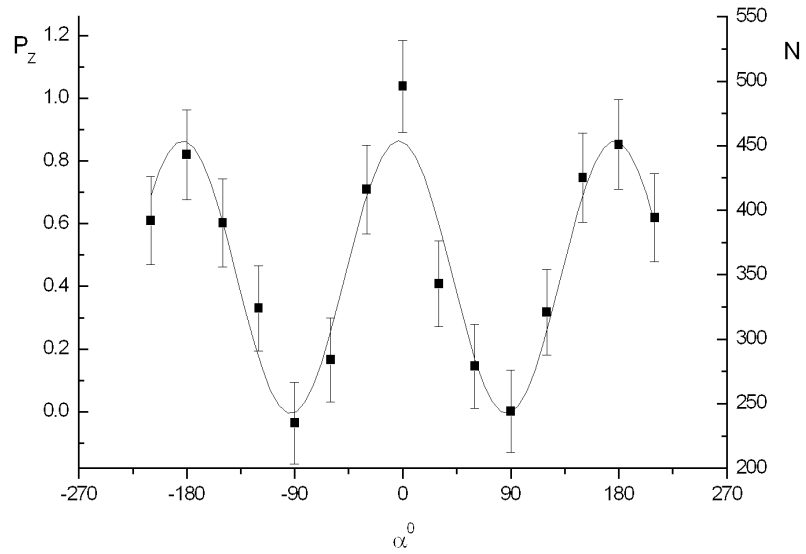


Figure 8: The dependence of the neutron intensity  $N$  on the angle  $\alpha^\circ$  between the Schwinger magnetic field  $\mathbf{H}_g^S$  and the vector of polarization of incident neutrons for the Bragg angle  $\theta_B = 84^\circ$ .

If the neutron spins turn round by the angles  $\pm\Delta\phi_0^S$  in the crystal for the waves described by  $\psi^{(1)}$  and  $\psi^{(2)}$ , the counting rate  $N$  of the neutrons after the analyzer will be:

$$N = N_0(1 + P_Z) = N_0(1 + P_0(\cos \Delta\phi_0^S \sin^2 \alpha + \cos^2 \alpha)), \quad (11)$$

where  $P_Z$  is the projection of a neutron polarization after the crystal on the direction  $\mathbf{H}_g^S$ . In the case of  $\Delta\phi_0^S = 0$  we will have  $P_Z \equiv P_0$  and  $N$  will not depend on the angle  $\alpha$ . The value of initial polarization was  $P_0 = (87 \pm 3)\%$  for neutrons with the wavelength  $\lambda \simeq 4.8\text{\AA}$ .

The example of the dependence  $N(\alpha)$  is shown in Fig. 8. The values of polarization  $P_Z$  are shown on the left axis of ordinates. The solid curve in Fig. 8 is a result of fitting the experimental points by the dependence (11).

As it has been noted earlier [8, 9], the angle of neutron spin rotation due to Schwinger interaction does not depend on the Bragg angle, and that is experimentally proved (see Fig. 9).

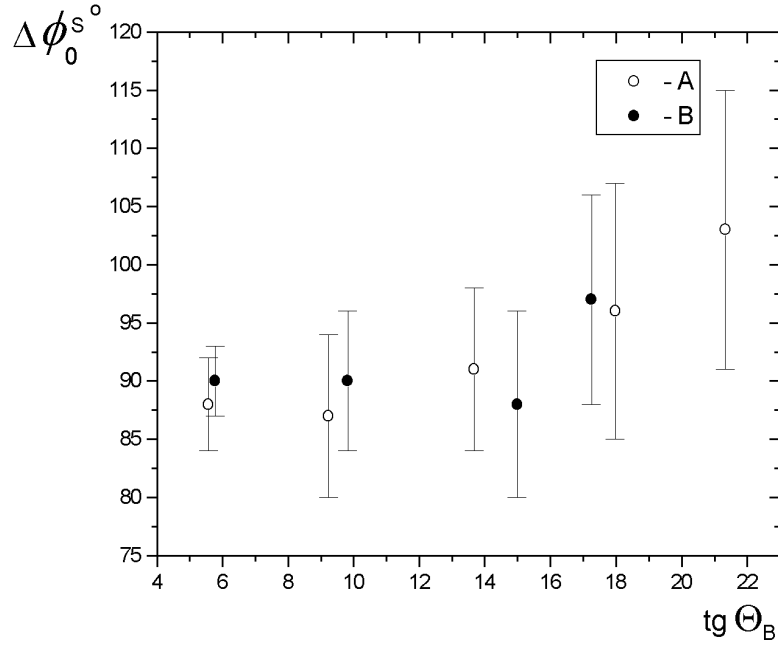


Figure 9: The dependence of the angle  $\Delta\phi_0^S$  of a neutron spin rotation due to Schwinger interaction on the tangent of Bragg angle. **A** and **B** are two crystal positions (see Fig. 2, and Fig. 4).

The experimentally observed result corresponds to the interplanar electric field, acting on a diffracted neutron, equal to

$$E_{(110)} = (2.24 \pm 0.05(0.20))10^8 \text{ V/cm}, \quad (12)$$

The systematic error caused by uncertainty of the contribution of background reflections is pointed in parentheses.

The experimental values are in good agreement with the earlier theoretical predictions and confirm the opportunity to increase more than by an order of magnitude the sensitivity of the method to neutron EDM, using the angles of diffraction close to  $90^\circ$ . It is experimentally shown that the value  $E\tau$  determining the sensitivity of the method in our case can reach  $\sim 0.2 \cdot 10^6$  V s/cm, what is comparable with that of the UCN method ( $\sim 0.6 \cdot 10^6$  V s/cm)[5] and much more than the value obtained by Shull and Nathans ( $\sim 0.2 \cdot 10^3$  V s/cm)[11].

## 5 Experimental test of the sensitivity

In 2002 the test experiment was carried out at ILL (Grenoble, France)[31]. The main purpose of this experiment was to estimate the statistical sensitivity of the Laue diffraction method for the neutron EDM, using the available quartz crystal and the facility for particle physics with cold polarized neutrons PF1A or PF1B at the ILL high flux reactor. The scheme of the experiment was similar to that of the previous one (see Fig. 4<sup>a</sup>). The TOF distance was  $\approx 1$  m. The experiment was carried out using the (110) plane ( $d=2.456\text{\AA}$ ) of a quartz crystal with the sizes  $14 \times 14 \times 3.5$  cm<sup>3</sup> prepared and tested at PNPI (Gatchina, Russia). The mosaicity of the crystal was less than 1" over all crystal volume.

Examples of experimental TOF spectra of the forward diffracted beam are shown in Fig.10. The positions and widths of the different reflection peaks coincide with the theoretical expectations.

One can see from Fig.10 that the reflection peaks are located on a background. Its spectrum is proportional to that of the incident beam. This background is due to incoherent scattering of the incident neutrons inside the crystal. It can be reduced essentially by increasing the distance between the crystal and detector (see Fig.11) and will be negligible for the final geometry of the experiment.

The measured dependencies of the time the neutrons stay inside the crystal are shown in Fig.12. The two curves correspond to the symmetric crystal positions A and B with the same Bragg angles, see Fig. 4<sup>a</sup>). The difference of these two curves is due to an inaccuracy of the initial angular position of the crystal. The time of stay reaches 1.8 ms for the Bragg angle  $\theta_B \approx 88.5^\circ$  which corresponds to the mean neutron velocity  $v_{\parallel} \approx 20$  m/s in the crystal. The incident neutron velocity was  $\approx 800$  m/s ( $\lambda \approx 5$  Å).

The dependence of the (110) reflection intensity on the Bragg angle is shown in Fig.13. One can see a good coincidence of the theory with the experimental data for Bragg angles smaller than  $86^\circ$ . The disagreement between theory and experiment for Bragg angles larger than  $87^\circ$  can be explained by the decrease of the area of the incident neutron beam "seen" by the crystal for large angles of diffraction.

These measurements allow us to determine the dependence of the statistical sensitivity for the neutron EDM on the Bragg angle (see Fig.14). This dependence has maximum for the Bragg angle equal to  $86^\circ$ .

Using the experimentally measured values of the time of neutron passage through the crystal (Fig.12), the intensity of the diffracted beam (Fig.13), and the previously measured value of the electric field for the (110) crystallographic plane ( $E_g = 2.2 \cdot 10^8$  V/cm [30, 32]) we can estimate the statistical sensitivity of this method to measure the neutron EDM, using the world's highest intensity cold neutron beam PF1B and the quartz crystal. This sensitivity is equal to  $\sim 6 \cdot 10^{-25}$  e · cm per day for the Bragg angle  $\theta_B = 86^\circ$ .

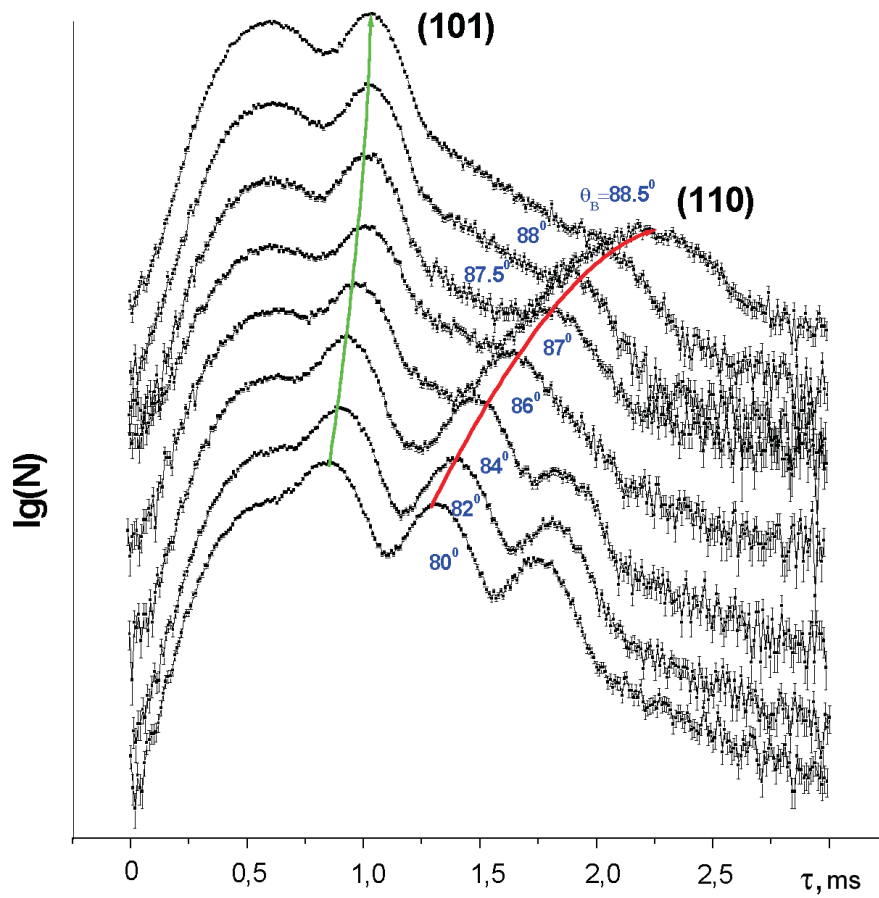


Figure 10: Spectrum of the forward diffracted neutron beam for different Bragg angles. Note the principal difference in the behavior of the working plane (110) and the other crystallographic planes (for instance, (101)).

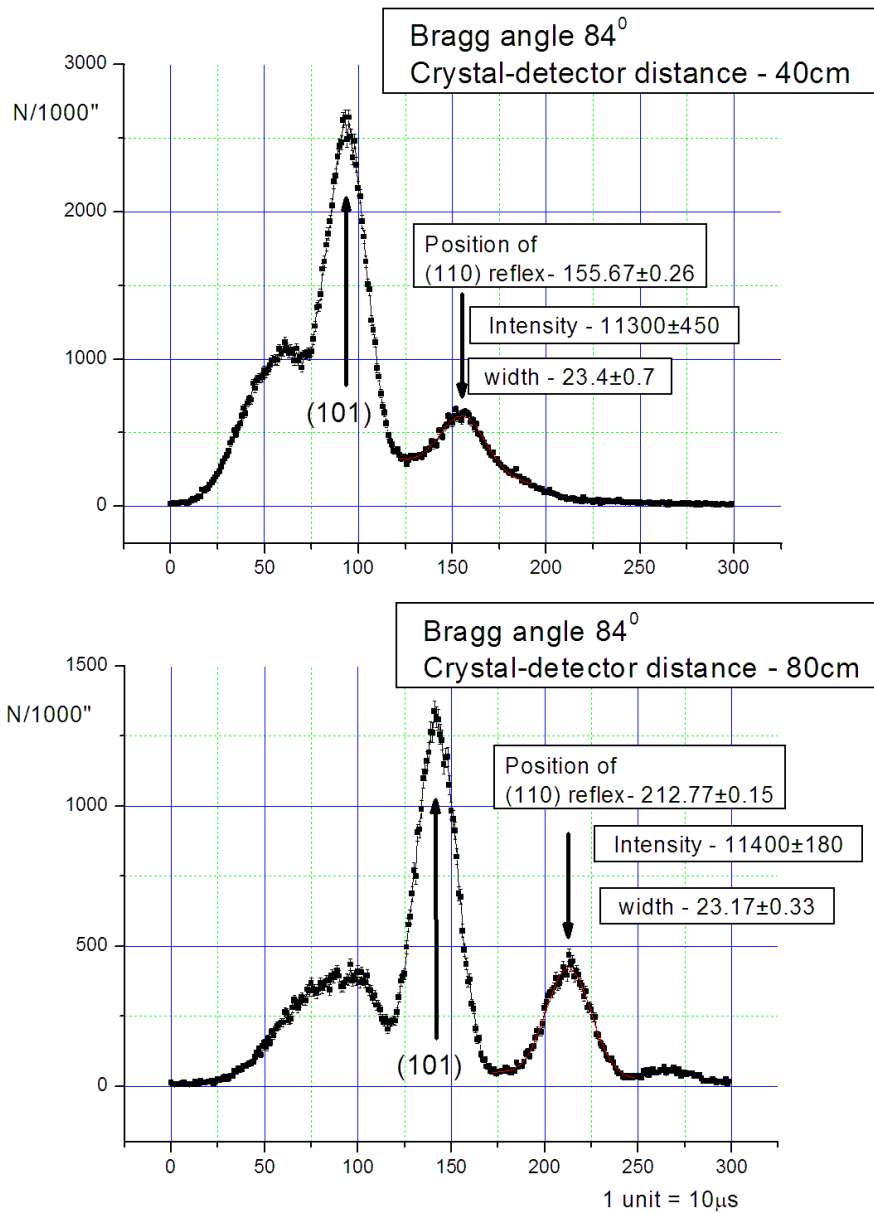


Figure 11: Spectrum of the forward diffracted neutron beam for two time of flight distances.



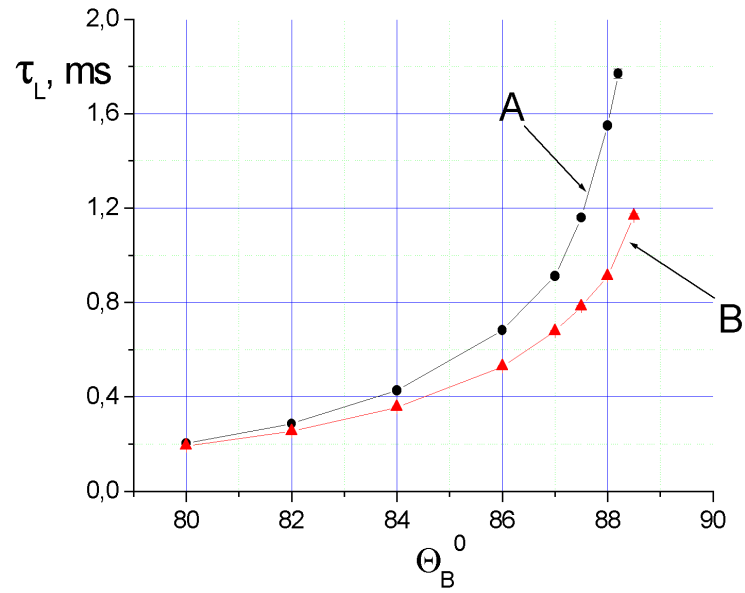


Figure 12: The dependence of the time of neutron stay in the crystal on the Bragg angle.

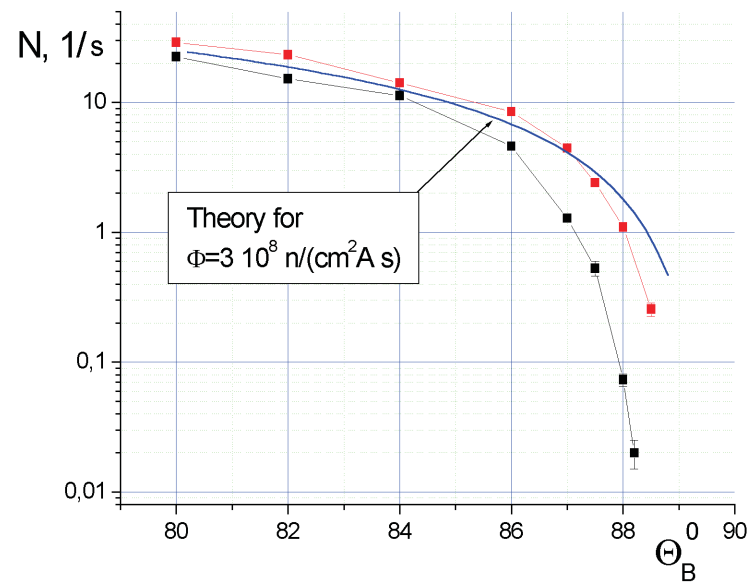


Figure 13: Dependence of the intensity of the (110) reflection of the quartz crystal on the Bragg angle. The two curves correspond to the symmetrical crystal positions A and B (see Fig. 4<sup>a</sup>).

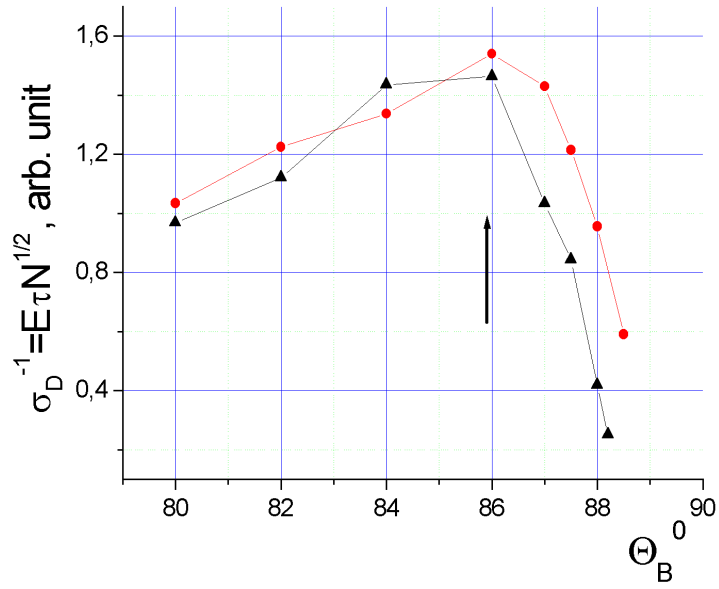


Figure 14: The measured dependence of the sensitivity of the method for the neutron EDM on the Bragg angle.

The comparison with the magnetic resonance method using ultracold neutrons (UCN-method) [3, 4, 5] is given in Table 1.

Possible further progress of this method for the neutron EDM search experiment may be associated with the use of some other crystals. In principle, there are the crystals that can allow to increase the method sensitivity about by an order of value in comparison with the quartz one (see Table. 2).

Table 1: The comparison of the Laue diffraction method with the UCN one. The intensity for the Laue diffraction scheme is recalculated from the experimental value (see Fig. 13) for the quartz crystal dimensions  $3.5 \times 14 \times 25 \text{ cm}^3$  and Bragg angle  $\theta_B = 86^\circ$  ( $\pi/2 - \theta_B \simeq 1/15$ ).

	UCN-method [5]	Laue diffraction method
$E$ (kV/cm)	4.5	$2.2 \cdot 10^5$
$t$ (s)	130 ( $v = 5\text{-}6 \text{ m/s}$ )	$0.7 \cdot 10^{-3}$ ( $v_{\parallel} \approx 50 \text{ m/s}$ )
$Et$ (kV s/cm)	585	150
$N$ (neutrons/s)	60	$1 \cdot 10^3$
$\sigma_D$ e-cm per day	$6 \cdot 10^{-25}$	$6 \cdot 10^{-25}$

Table 2: Parameters of some noncentrosymmetric crystal suitable for the EDM experiment.  $\tau_a$  is a time of neutron life in the crystal (time of absorption).

Crystal	Group Symmetry	$hkl$	$d$ , (Å)	$E_g$ , $10^9 \text{ V/cm}$	$\tau_a$ , ms	$E_g \tau_a$ , (kV s/cm)
$\alpha$ -quartz (SiO <sub>2</sub> )	$32(D_3^6)$	111	2.236	0.23	1.0	230
		110	2.457	0.20		220
Bi <sub>12</sub> SiO <sub>20</sub>	123	433	1.75	0.43	4.0	1720
		312	2.72	0.22		880
Bi <sub>4</sub> Si <sub>3</sub> O <sub>12</sub>	$-43m$	242	2.1	0.46	2	920
		132	2.75	0.32		640
PbO	$Pca21$	002	2.94	1.04	1	1040
		004	1.47	1.0		1000
BeO	$6mm$	011	2.06	0.54	7.0	3700
		201	1.13	0.65		4500

## 6 Neutron optics in noncentrosymmetric crystal

Here we consider the neutron-optic effects for a neutron, moving through a noncentrosymmetric crystal with the energy and direction far from the Bragg ones, when the deviation from the exact Bragg condition reaches  $(10^3 - 10^5)$  Bragg widths.

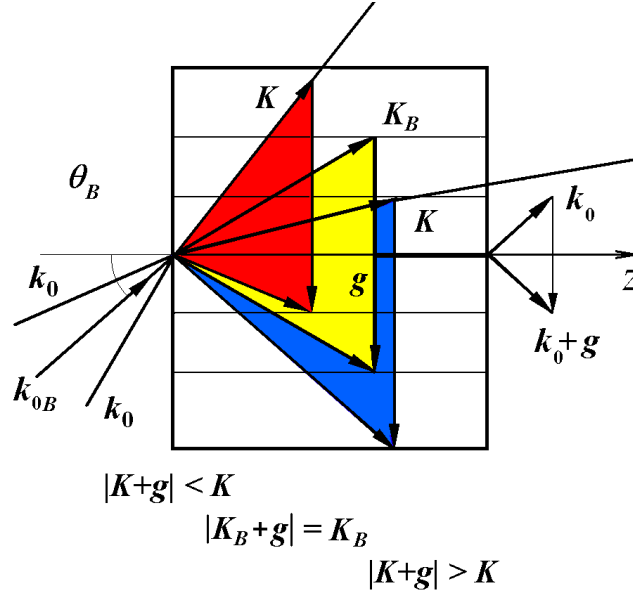


Figure 15: Neutron movement with the different directions of the wave vectors  $\mathbf{K}$  with the respect to reciprocal lattice vector  $\mathbf{g}$ . a)  $|\mathbf{K} + \mathbf{g}| > K$ , neutrons are concentrated at the "nuclear planes" (maxima of nuclear potential). b)  $|\mathbf{K} + \mathbf{g}| < K$ , neutrons are concentrated between the "nuclear planes". These two cases correspond to neutron optics. c) The third case  $|\mathbf{K} + \mathbf{g}| = K$  corresponds to the neutron diffraction, when the both kinds of waves excite in the crystal.

The essence of the phenomenon is the following. Let a neutron is moving through the crystal and the Bragg condition is not satisfied for any crystallographic plane. In this case the distribution of the neutron density  $|\psi(\mathbf{r})|^2$  in the crystal can be written using a perturbation theory [33]:

$$|\psi(\mathbf{r})|^2 = 1 + \sum_g \frac{2v_g}{E_k - E_{k_g}} \cos(\mathbf{g}\mathbf{r} + \phi_g). \quad (13)$$

where  $E_k = \hbar^2 k^2 / 2m$  and  $E_{k_g} = \hbar^2 |\mathbf{k} + \mathbf{g}|^2 / 2m$  are the energies of the neutron with the wave vectors  $\mathbf{k}$  and  $\mathbf{k} + \mathbf{g}$  in the crystal, the values  $v_g$  and  $\phi_g$  are respectively the absolute magnitude and the phase of the  $g$ -harmonics amplitude  $V_g = v_g \exp i\phi_g$  of the neutron crystal interaction potential, which has a form

$$V(\mathbf{r}) = \sum_g V_g \exp i(\mathbf{g}\mathbf{r}) = V_0 + \sum_g 2v_g \cos(\mathbf{g}\mathbf{r} + \phi_g), \quad (14)$$

difference  $\Delta_g = E_k - E_{k_g}$  describes the deviation from the Bragg condition measured in the energy units. One can see that the neutrons are concentrating either on the maxima or on the minima of the periodic potential, depending on the sign of  $\Delta_g$  (see Fig. 15,16), the degree of this concentration being determined by the value of  $v_g/\Delta_g$ .

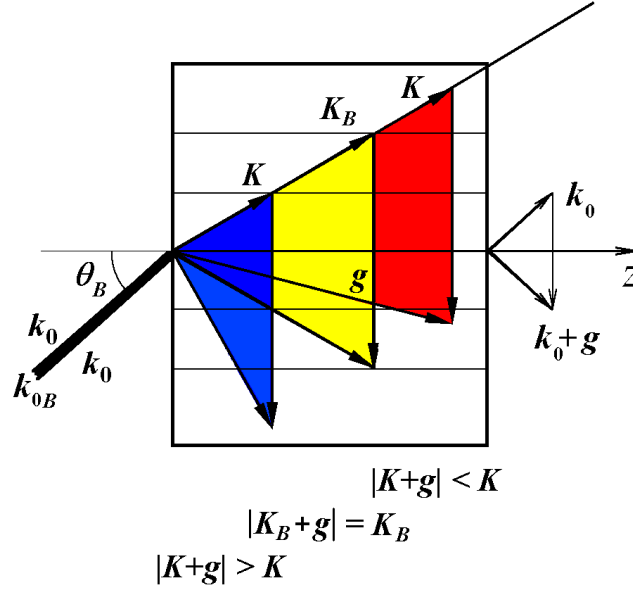


Figure 16: Neutron movement with the different absolute values of the wave vectors  $\mathbf{K}$  (different wave lengths). The same three cases as in the Fig. 15  $|\mathbf{K} + \mathbf{g}| > K$ ,  $|\mathbf{K} + \mathbf{g}| < K$  and  $|\mathbf{K} + \mathbf{g}| = K$

The neutron interacts with the nonmagnetic crystal by the nuclear forces, therefore the neutrons will concentrate on the maxima (or on the minima) of the *nuclear* crystal potential, so the neutrons in the noncentrosymmetric crystal will move under electric interplanar field as in the diffraction case analyzed above. The sign of the electric field depends on the sign of the deviation parameter  $\Delta_g = E_k - E_{k_g}$ .<sup>6</sup>

Due to such concentration the neutron kinetic energy in the crystal  $E_k = \hbar^2 k^2/2m$  (in the second order of the perturbation theory) will be equal to

$$\frac{\hbar^2 k^2}{2m} = \frac{\hbar^2 k_0^2}{2m} - V_0 - \sum_g \frac{V_g V_{-g}}{\Delta_g} \equiv \frac{\hbar^2 K^2}{2m} - \sum_g \frac{V_g V_{-g}}{\Delta_g}, \quad (15)$$

where  $k_0$  is the wave vector of an incident neutron and  $k$  is the wave vector of the neutron in the crystal,  $K$  is the wave vector in the crystal with the mean nuclear potential  $V_0$  taken into account  $\hbar^2 K^2/2m = \hbar^2 k_0^2/2m - V_0$ . As follows from (15), the neutron, moving through the crystal far from the Bragg directions, nevertheless, "feels" the crystal structure.

<sup>6</sup>The equality  $E_k = E_{k_g}$  corresponds to exact Bragg condition for the plane system  $\mathbf{g}$ . In this case the perturbation theory (valid for  $v_g \ll (E_k - E_{k_g})$ ) becomes inapplicable, and one should use the two wave diffraction theory.

For the case of non-magnetic and non-absorbing crystal the expression for  $V_g$  can be written as [33]:

$$V_g = v_g^N e^{i\phi_g^N} + iv_g^E e^{i\phi_g^E} \mu \frac{\boldsymbol{\sigma}[\mathbf{g} \times \mathbf{v}]}{c}, \quad (16)$$

where  $v_g^N, \phi_g^N$  are respectively the absolute magnitude and the phase of the  $g$ -harmonics amplitude of the nuclear neutron-crystal potential,  $v_g^E, \phi_g^E$  are the absolute magnitude and the phase of the  $g$ -harmonics amplitude of the electric potential of crystal,  $\mu, v$  are the magnetic moment and the velocity of neutron,  $c$  is the light speed.

By substituting this expression into (15) and taking into account that for non-absorbing crystal  $V_g = V_{-g}^*$ , we shall obtain

$$\frac{\hbar^2 k^2}{2m} = \frac{\hbar^2 K^2}{2m} - \sum_g \frac{(v_g^N)^2}{\Delta_g} - \mu \frac{\boldsymbol{\sigma}[\mathbf{E}_{sum} \times \mathbf{v}]}{c}, \quad (17)$$

where

$$\mathbf{E}_{sum} = \sum_g \frac{2v_g^N}{\Delta_g} v_g^E \mathbf{g} \sin(\Delta\phi_g) \quad (18)$$

is a resultant electric field affecting a neutron in the crystal. Here  $\Delta\phi_g \equiv \phi_g^N - \phi_g^E$  is the phase shift between  $g$ -harmonics of nuclear and electric potentials of the crystal.

We should note that the neutron refraction index  $n$  in this case will depend on the neutron spin direction

$$n^2 = k^2/k_0^2 = n_0^2 - \Delta n_d^2 - \Delta n_s^2, \quad (19)$$

where  $n_0^2 = K^2/k_0^2$  is a square of a mean refraction index for neutron in the crystal,

$$\Delta n_d^2 = (2m/\hbar^2 k_0^2) \sum_g (v_g^N)^2 / \Delta_g \quad (20)$$

is a small diffraction correction to the square of mean refraction index,

$$\Delta n_s^2 = (2m/\hbar^2 k_0^2) (\mu \boldsymbol{\sigma}[\mathbf{E}_{sum} \times \mathbf{v}]) / c \quad (21)$$

is a spin dependent correction arisen due to interference of nuclear and electric amplitudes.

For the centrosymmetric crystal  $\Delta\phi_g \equiv 0$  and therefore  $\mathbf{E}_{sum} \equiv 0$ . In the noncentrosymmetric crystals there are the crystallographic planes, for which  $\Delta\phi_g \neq 0$  and so the electric field acting on a neutron will be nonzero  $\mathbf{E}_{sum} \neq 0$ .

Therefore a spin dependence arises for the neutron-crystal interaction, which leads to different values of a neutron wave vector in the crystal for two opposite spin orientations that in turn leads to neutron spin rotation around the direction of Schwinger magnetic field  $\mathbf{H}_{sum}^S = [\mathbf{E}_{sum} \times \mathbf{v}] / c$ .

The rotation angle for the crystal length  $L$  will be equal

$$\Delta\varphi_s = \frac{2\mu}{\hbar} \frac{\boldsymbol{\sigma}[\mathbf{E}_{sum} \times \mathbf{v}]}{c} \frac{L}{v}. \quad (22)$$

One should add an imaginary part into the nuclear crystal potential to describe the absorbing crystal:

$$V_g = v_g^N e^{i\phi_g^N} + iv_g^{N'} e^{i\phi_g^{N'}} + iv_g^E e^{i\phi_g^E} \mu \frac{\boldsymbol{\sigma}[\mathbf{g} \times \mathbf{v}]}{c}. \quad (23)$$

Here  $v_g^{N'}$ ,  $\phi_g^{N'}$  are the amplitude and phase of  $g$ -harmonics of the imaginary part of the nuclear potential.

The value of kinetic energy in the crystal becomes equal to:

$$\frac{\hbar^2 k^2}{2m} = \frac{\hbar^2 K^2}{2m} - V_{(g)} - i(V_0' + V_{(g)}') - \mu \frac{\boldsymbol{\sigma}[(\mathbf{E}_{sum} + i\mathbf{E}'_{sum}) \times \mathbf{v}]}{c}, \quad (24)$$

where

$$V_{(g)} = \sum_g \frac{(v_g^N)^2 - (v_g^{N'})^2}{\Delta_g}, \quad (25)$$

$$V_{(g)}' = \sum_g \frac{2v_g^N v_g^{N'} \cos(\phi_g^N - \phi_g^{N'})}{\Delta_g}, \quad (26)$$

$$\mathbf{E}'_{sum} = \sum_g \frac{2v_g^{N'}}{\Delta_g} v_g^E \sin(\phi_g^{N'} - \phi_g^E) \mathbf{g}. \quad (27)$$

The estimations give that the values of the diffraction corrections to a mean potential for  $\alpha$ -quartz crystal are  $V_{(g)} + iV_{(g)}' \approx 10^{-3}(V_0 + iV_0')$ ,  $\mu\boldsymbol{\sigma}[(\mathbf{E}_{sum} + i\mathbf{E}'_{sum}) \times \mathbf{v}]/c \approx 10^{-6}(V_0 + iV_0')$  for the wide range of the incident neutron wavelengths and sharply increase near the Bragg conditions. We should note also that in spite of a smallness the last correction leads to relatively large and observable effects due to its spin dependence.

## 7 Observation of the neutron spin rotation

The experiment was carried out at the PNPI WWR-M reactor. Scheme of the experiment is shown in Fig. 17, see [34, 35, 29].

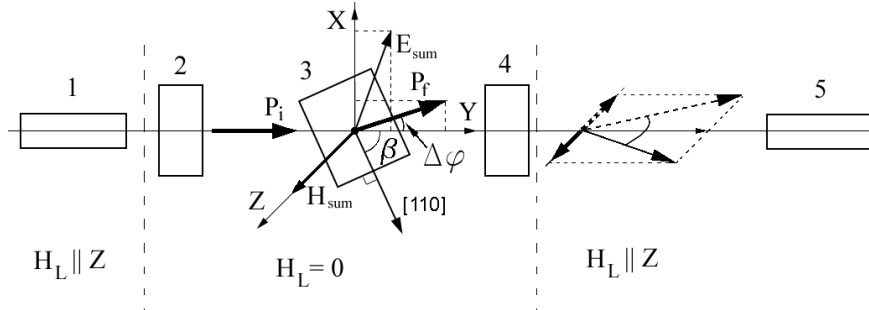


Figure 17: Scheme of the experiment. 1 is a polarizer; 2 is a  $\pi/2$  coil to turn spin around X axis; 3 is the  $\alpha$ -quartz single crystal with the sizes  $14 \times 14 \times 3.5$  cm<sup>3</sup>; 4 is a  $\pm\pi/2$  coil to turn around Y axis; 5 is an analyzer.  $\mathbf{H}_L$  is the guiding magnetic field;  $O$  is an axis (parallel to Z direction) of a crystal rotation;  $\mathbf{P}_i$  and  $\mathbf{P}_f$  are the polarizations of neutron beam before the crystal and after it.

Initially the neutron spin was directed along the neutron velocity (axis Y). The X-component of the polarization was measured after neutron passage through the crystal. This component should be equal to zero, if the spin rotation effect is absent. Time of flight technique was used for measuring the spectral dependence of polarization. The crystal was overturned around Z axis to eliminate the false effect due to nonzero value of the X-component of polarization for real setup. The effect changes its sign due to a change of the sign of the electric field in this case.

The measurement was carried out using the  $\alpha$ -quartz crystal with the dimensions  $14 \times 14 \times 3.5 \text{ cm}^3$ . The crystal orientation was determined by the angle  $\beta$  between the neutron velocity (Y axis) and the [110] crystal axis.

The theoretical dependence of the angle of neutron spin rotation  $\Delta\varphi_s$  on the value and direction of neutron wavevector is shown in Fig. 18.

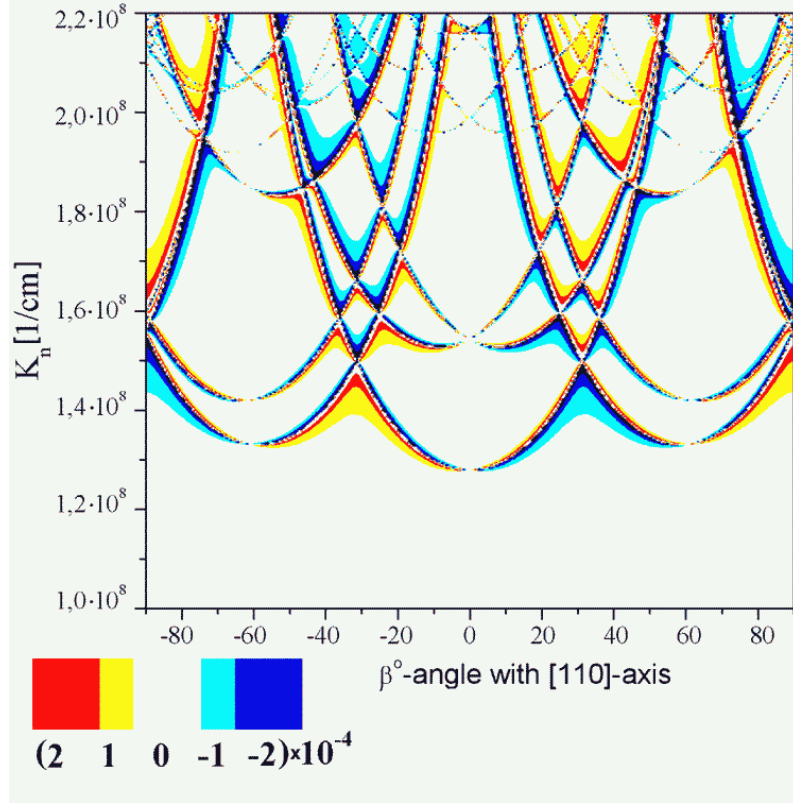


Figure 18: Theoretical dependence of  $\Delta\varphi_s$  on the wavevector and direction of neutron for the  $\alpha$ -quartz crystal.

The experiment was carried out for two crystal positions with  $\beta = 90^\circ$  and  $30^\circ$ . The results are shown in Figs. 19, 20. Two plots at the figures correspond to different energy resolution of the experiment ( $\Delta\lambda/\lambda = 5 \cdot 10^{-2}$  and  $= 2 \cdot 10^{-2}$ ). The solid curves reproduce the theoretical dependence (22) averaged over energy resolution. The dotted lines indicate



the positions of the crystallographic planes with nonzero value of  $\Delta\phi_g$  (see (18)). One can see a good agreement between theoretical and experimental results. The resultant electric field  $|\mathbf{E}_{sum}|$  is shown on the right ordinates axis. Its value is  $|\mathbf{E}_{sum}| \approx (1 - 10) \cdot 10^4$  V/cm for any point of spectrum, and so  $\Delta\varphi_s$  may reach  $\pm 2 \cdot 10^{-4}$  rad/cm.

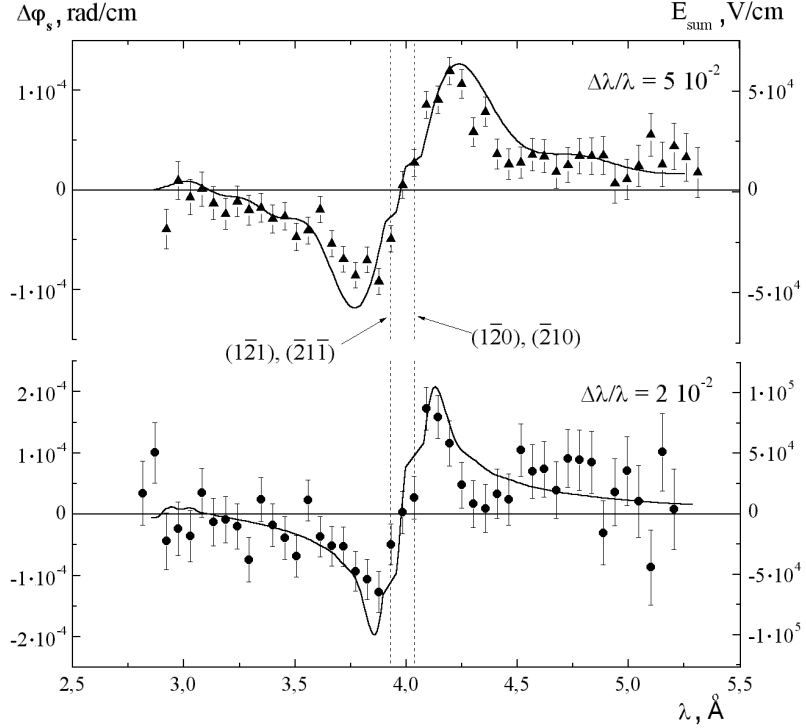


Figure 19: Energy dependence of  $\Delta\varphi_s$  for  $\beta = 90^\circ$ . Solid curves are the theoretical dependence (22) after averaging over the energy resolution of the experiment.

## 8 Spin rotation effect for Bragg reflected neutrons from the deformed crystal part

In the previous chapter we have considered the effect of neutron spin rotation for large deviations from exact Bragg condition ( $\sim 10^3 - 10^4$  Bragg width). The measured effect has coincided with the theoretical one but has a small value [35]. Here we consider the situation when we can tune the sign and value of the deviation from the exact Bragg condition within a few Bragg width. In this case the neutron spin rotation angle essentially increases due to increasing the electric field affected the neutron.

Let's consider the symmetric Bragg diffraction scheme with the Bragg angles close to the right one. Neutrons fall on the crystal in the given direction with the energy close to the Bragg one for the crystallographic plane  $g$ . Deviation from the exact Bragg condition is

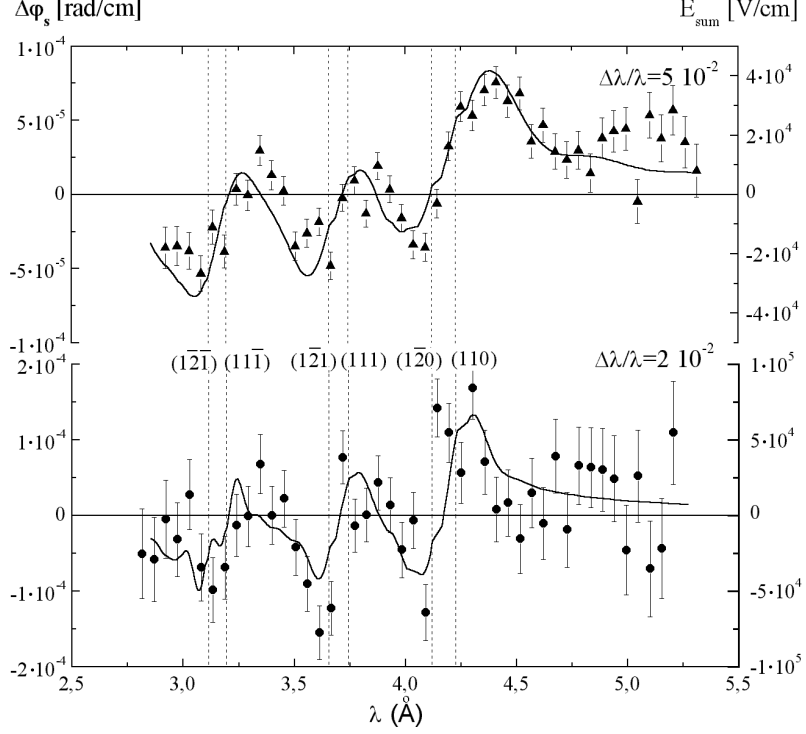


Figure 20: Energy dependence of  $\Delta\varphi_s$  for  $\beta = 30^\circ$ .

described by the parameter  $\Delta_g = E_k - E_{k_g}$ , where  $E_k = \hbar^2 k^2 / 2m$  and  $E_{k_g} = \hbar^2 |\mathbf{k} + \mathbf{g}|^2 / 2m$  are the energies of a neutron in the states  $|k\rangle$  and  $|k + g\rangle$  respectively.

In this case the neutron wave function inside the crystal in the first order of perturbation theory can be written [33]

$$\psi(\mathbf{r}) = e^{-i\mathbf{k}\mathbf{r}} + a \cdot e^{-i(\mathbf{k}+\mathbf{g})\mathbf{r}}, \quad (28)$$

where

$$a = \frac{|V_g|}{E_k - E_{k_g}} = \frac{|V_g|}{\Delta_g}. \quad (29)$$

Here  $V_g$  is  $g$ -harmonic of interaction potential of neutron with crystal. For simplicity we consider the case  $a \ll 1$ , so we can use the perturbation theory.

The electric field affected the diffracted neutron will be equal to [33]

$$\mathbf{E} = 2\mathbf{E}_g \cdot a, \quad (30)$$

where  $\mathbf{E}_g$  is the interplanar electric field for the exact Bragg condition.

One can see that the sign and value of the electric field (30) are determined by the sign and value of deviation  $\Delta_g$  from the exact Bragg condition, therefore to have the given electric field and so the effect of neutron spin rotation we should select from the whole beam the neutrons with the corresponding deviation parameter  $\Delta_g$ .

The presence of the electric field will lead to an appearance of the Schwinger magnetic field

$$\mathbf{H}_S = 1/c[\mathbf{E} \times \mathbf{v}_{\parallel}]. \quad (31)$$

The neutron spin will rotate around the  $\mathbf{H}_S$  by the angle

$$\varphi_s = \frac{4\mu H_S L_c}{\hbar v_{\perp}}, \quad (32)$$

$L_c$  is the crystal thickness,  $v_{\parallel}$  and  $v_{\perp}$  are the components of neutron velocity parallel and perpendicular to the crystallographic plane correspondingly.

The main idea of the experiment is the following. We use a small controlled variation of the interplanar distance  $\Delta d$  (caused by heating, for example) near the exit crystal edge. So some part of neutrons passed through the crystal will reflect from this small crystal part. These back diffracted neutrons have the deviation parameter for the main part of crystal determined by  $\Delta d$  and so they propagate under corresponding electric field in both directions there and back. Thermal deformation of the crystal edge is used to create such variation of the interplanar distance.

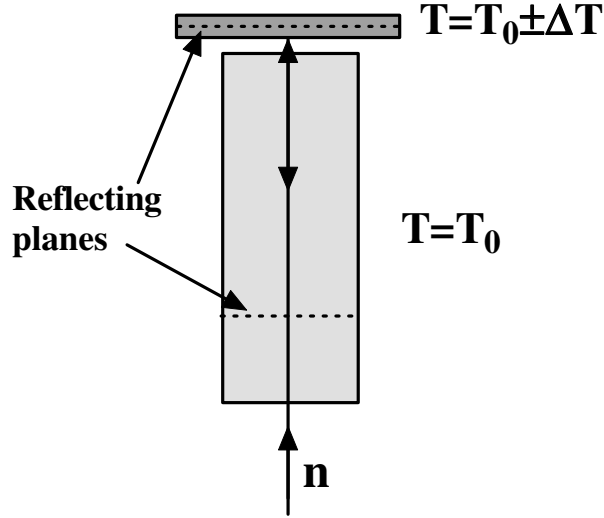


Figure 21: Two crystals are in parallel position. Neutron reflected by the small crystal pass twice through the large crystal. The deviation parameter  $\Delta_g$  for the large crystal is determined by the temperature difference  $\Delta T$ .

We can use also two separate crystals in parallel position for this purpose (see Fig.21). One can heat (or cool) the second small crystal. The part of neutrons passed through the first crystal with the corresponding Bragg wave length will reflect by the second crystal with the given deviation parameter for the first (large) crystal. This deviation parameter will directly depend on the temperature difference between crystals.

Value of the wave length Bragg width for (110) quartz plane ( $d = 2.45\text{\AA}$ ) is  $\Delta\lambda_B/\lambda \approx 10^{-5}$ . To shift the wave length of the reflected neutrons by the one Bragg width we should

heat (or cool) the second crystal to have the same value of  $\Delta d/d$ . Linear coefficient of the thermal expansion for quartz crystal is  $\Delta L/L \approx 10^{-5}$  per degree. Therefore, the deviation  $\pm \Delta \lambda_B$  corresponds to difference of the crystal temperatures  $\Delta T \approx \pm 1^0$ . We note that the different signs of this temperature difference will correspond to different signs of the electric field acting on the neutron.

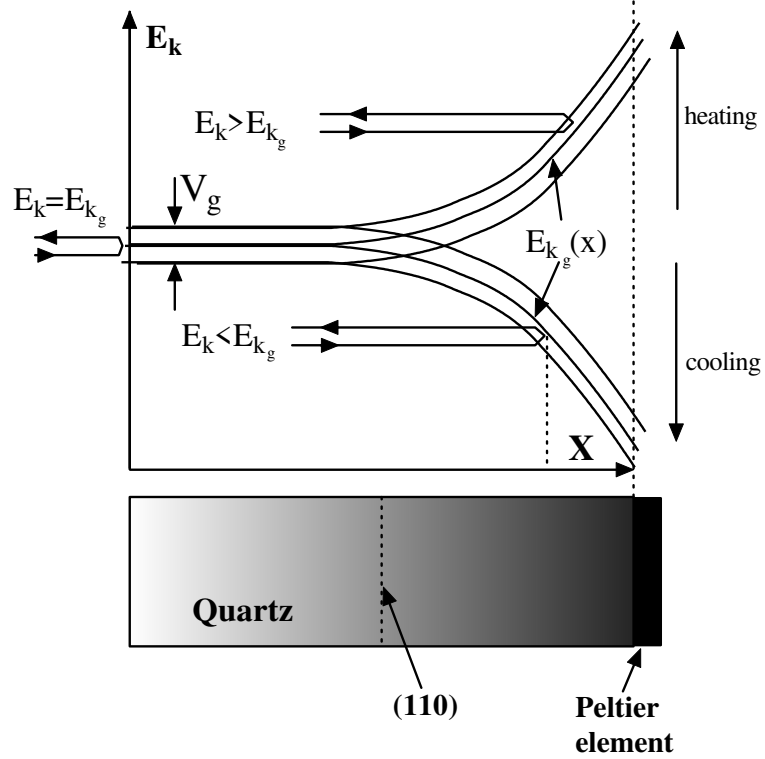


Figure 22: Passage of the neutron through the crystal. Presence of the interplanar distance gradient result in forming the reflex near the back face of crystal.

Scheme of the neutron behavior in the crystal is shown in Fig.22. Two samples of quartz crystal has been used in this experiment with the thicknesses along  $X$  axis  $L_c = 14$  and  $27$  cm. The Peltier element has been attached to the back face of the crystal. That allows to create the temperature gradient in the crystal along the neutron trajectory. So the Bragg condition will vary along the neutron trajectory and different parts of crystal reflect the neutrons with the different  $\lambda$ . Therefore, the reflected beam will contain not only the reflex from the entrance crystal face (corresponding to Bragg condition for  $d$ ) but also the reflection from the back exit face (corresponding  $d \pm \Delta d$ ) that twice pass through the crystal there and back. Moreover, the value of the deviation parameter  $\Delta_g$  for this reflection is directly depend on the value of temperature gradient. In the case of higher temperature of the back crystal face the neutron with  $E_k - E_{k_g} > 0$  will be reflected, while in the case of its lower temperature the neutron with  $E_k - E_{k_g} < 0$  will be reflected.

Examples of the time of flight spectra of the reflected neutrons for the Bragg angle  $\sim 90^\circ$  are shown in Fig.23. One can see a formation of the reflex from the back crystal surface and increasing its intensity with the rise of the temperature gradient.

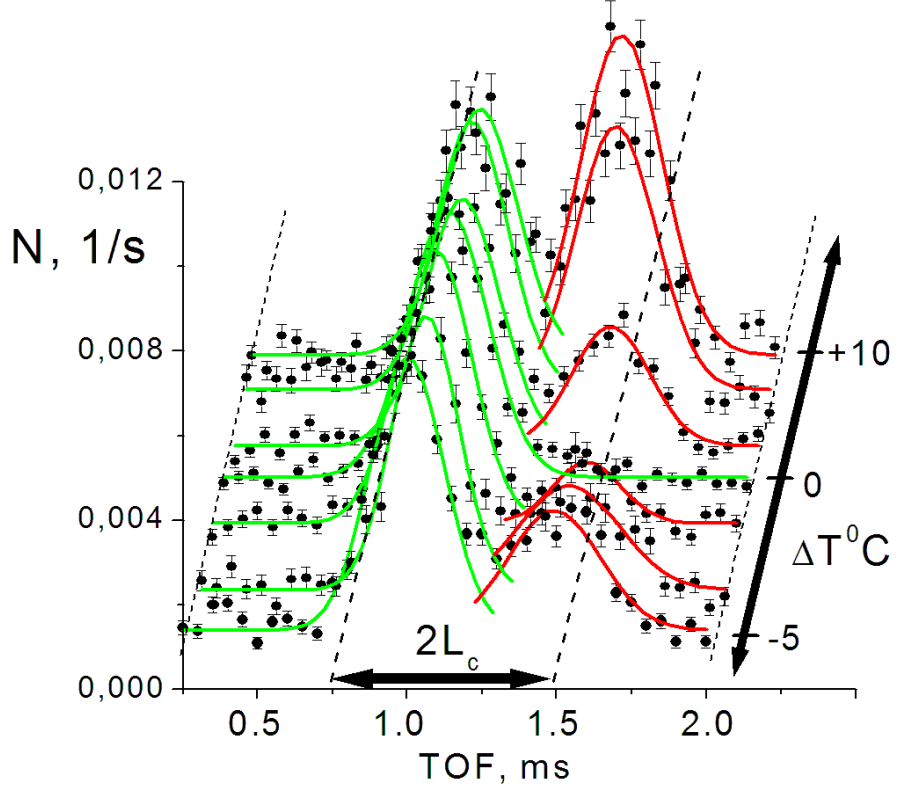


Figure 23: Dependence of the time of flight (TOF) spectra of the neutron reflected by the (110) plane of quartz on the temperature gradient applied to the crystal. Bragg angle  $\sim 90^\circ$ ,  $L_c = 27$  cm. One can see the reflexes from the front surface and from the back part of crystal.

The scheme of the experiment on the observation of neutron spin rotation is similar to that described in [32].

To observe the effect of neutron spin rotation due to Schwinger interaction it is necessary to turn the crystal in a position, for which Bragg angle is different from  $90^\circ$ , because in the case of Bragg diffraction the Schwinger effect disappears for  $90^\circ$  Bragg angle:

$$\varphi_s = \frac{4\mathbf{E}\mu L_c v_{\parallel}}{c\hbar v_{\perp}} = \frac{4\mathbf{E}\mu L_c}{c\hbar} ctg(\theta_B) \xrightarrow{\theta_B \rightarrow \pi/2} 0 \quad (33)$$

The experiment on the observation of neutron spin rotation was carried out with the  $L_c = 14$  cm crystal thickness and Bragg angle  $\approx 86^\circ$ .

The dependence of the angle of neutron spin rotation around  $\mathbf{H}_S$  on the value of temperature gradient is shown in Fig.24.

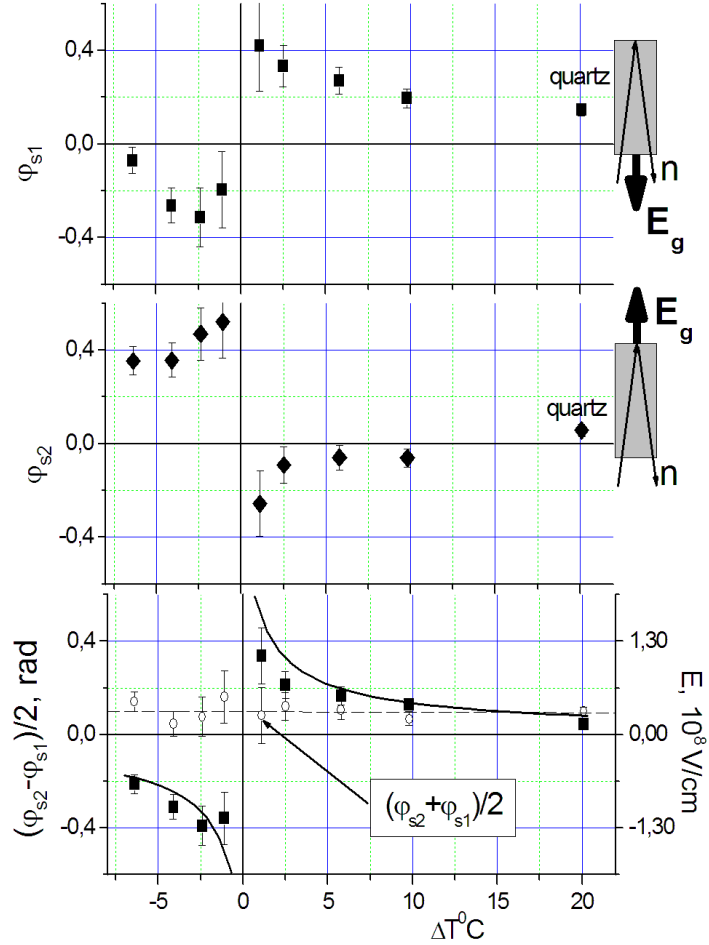


Figure 24: The dependence of the angle of neutron spin rotation due to Schwinger interaction on the value of temperature gradient. Two upper figure corresponds to two crystal positions differing by the angle  $180^\circ$ . One can see a good coincidence of the theoretical dependence (solid curve in the bottom plot) with the experimental points.

We can change the sign of the effect by turn the crystal by the  $180^\circ$  around  $\mathbf{H}_S$ . One can see that the experiment confirms that such a crystal rotation indeed change the sign of the observed effect. On the right axis the effective electric field that is necessary to get the corresponding spin rotation effect is shown. One can see that the value of the electric field reaches  $\sim 1.3 \cdot 10^8$  V/cm, that is only 1.5 times less than in the Laue diffraction case for exact Bragg condition [7, 30].

## 9 Conclusion

The first experimental study of some new phenomena for the neutron diffraction and optics in the noncentrosymmetric crystal was carried out, using the pilot set-up created for a search for the neutron EDM by the crystal-diffraction method.

For the first time the neutron dynamical Laue diffraction for the Bragg angles close to the right one (up to  $87^\circ$ ) was studied, using the forward diffraction beam and the thick ( $\sim 3.5$  cm) crystal.

The effect of the essential time delay of diffracting neutrons inside the crystal for Bragg angles close to  $90^\circ$  was experimentally observed. For (110)-plane of  $\alpha$ -quartz and  $\theta_B = 88.5^\circ$  we have obtained  $\tau_L \approx 1.8$  ms that corresponds to  $v_{\parallel} \approx 20$  m/s, while  $v = 808$  m/s.

The predicted earlier phenomenon of the neutron beam depolarization was first experimentally observed for the case of Laue diffraction in the noncentrosymmetric  $\alpha$ -quartz crystal. It is experimentally proved that the interplanar electric field, affecting the neutron in the crystal, maintains its value up to Bragg angles equal to  $87^\circ$ .

It is shown experimentally that the value  $E\tau$  determining the sensitivity of the method in our case can reach  $\sim 2 \cdot 10^5$  V s/cm that is comparable with that for the UCN method ( $\sim 6 \cdot 10^5$  V s/cm)[5] and much more than the value obtained by Shull and Nathans ( $\sim 2 \cdot 10^2$  V s/cm)[11] and also than that of [36] ( $\sim 1.2 \cdot 10^3$  V s/cm)<sup>7</sup>.

These results give the opportunity to try the Laue diffraction method for a neutron EDM search. The statistical sensitivity of the method was estimated experimentally to be  $\sigma(D) \approx 6 \times 10^{-25}$  e · cm per day for the PF1B beam of the ILL reactor and available quartz crystal. The measured intensities and the neutron time of stay in the quartz crystal coincide well with the theoretical predictions. The use of the other crystals may allow to improve the sensitivity of the method by about one order of magnitude and to reach  $\sim$  a few  $10^{-26}$  e · cm per day.

The effect of a spin rotation due to Schwinger interaction of the magnetic moment of moving neutron with an interplanar electric field of the noncentrosymmetric crystal was experimentally observed for neutron, passing through the crystal far from the Bragg conditions.

The energy dependence of a spin rotation angle was measured for two crystal orientations. The dependence has a pronounced resonance form. The direction of a spin rotation changes its sign when the energy passes through the Bragg resonance value. So a new kind of neutronography arises for noncentrosymmetric crystals, which allows to "see" and study the crystallographic planes with nonzero electric interplanar fields.

For  $\alpha$ -quartz crystal the value of the spin rotation angle can reach  $\pm(1-2) \cdot 10^{-4}$  rad/cm that corresponds to the value of resultant electric field equal to  $\pm(0.5-1) \cdot 10^5$  V/cm.

We note also that the presence of the terms (26) and (27) in equation (24) should result in the dependence of a neutron absorption on the direction and the value of a neutron wave vector as well as on the neutron spin orientation.

The effect of spin rotation in a noncentrosymmetric quartz crystal for neutrons Bragg reflected by the deformed part of crystal was first observed. This effect is caused by the

---

<sup>7</sup>One can consider the measurements of the depolarization as a first preliminary and rough measurements of a neutron EDM, which gives the result  $D < 10^{-22}$  e · cm that is some better than the old Shull's and Nathans's result [11]. The result obtained in magnetic resonance method using cold neutrons [36] was  $D < 3 \cdot 10^{-24}$  e · cm.

Schwinger interaction and depends on a deformation degree of crystal near its back surface. For the quartz crystal the effective electric field affected the neutron during the time of its staying inside the crystal can reach  $\sim 1.3 \cdot 10^8$  V/cm. Simple estimation has shown that in our case the depth of neutron penetration into the crystal and so the time of neutron interaction with the electric field can be about four or even five orders more than in the well known Shull and Nathans experiment for the neutron EDM search [11].

In addition, the requirements to the crystal perfection are relatively low for this scheme. For the case  $\gamma_B \ll w_m$  the effective electric field affected the neutron depends on an effective crystal mosaicity  $w_m$  as  $E = E_0(\gamma_B/w_m)$ , where  $\gamma_B$  is the angular Bragg width, but the reflex intensity increase as  $I = I_0(w_m/\gamma_B)$ , therefore the sensitivity to measure the neutron EDM will be reduced only by a factor  $\sqrt{w_m/\gamma_B}$ , that give us a hope that such a scheme can be applied to search the T-odd part of neutron-nuclei interaction [21] using neutrons with energies near the P wave resonance one.

The authors are grateful to all our colleagues E.G. Lapin, E. Lelievre-Berna, V. Nesvizhevsky, A. Petoukhov, S.Yu. Semenikhin, T. Soldner, F. Tasset for numerous and useful discussions and for the active participation in the experiments.

This work is supported by RFBR: grants N 03-02-17016, 05-02-16241, by INTAS: grant N 00-00043.

## References

- [1] Khriplovich, I.B.; Lamoreaux, S.K. *CP Violation without Strangeness. The Electric Dipole Moments of Particles, Atoms and Molecules*; Springer-Verlag; 1996.
- [2] Bunakov, V.E. *Fiz. Elem. Chast. Atom. Yad. (EChAYa)* 1995 **26** 285–361. (in russian)
- [3] Altarev, I.S.; Borisov, Yu.V.; Borovikova, N.V.; et al. *Yad.Fiz.* 1996 **59** 1204.
- [4] Smith, K.F.; Crampin, N.; Pendlebury, J.M.; et al. *Phys. Lett.* 1990 **B234** 191.
- [5] Harris, P.G.; Baker, C.A.; Green, K.; et al. *Phys. Rev. Lett.* 1999 **82** 904.
- [6] Fedorov, V.V.; Voronin, V.V. *Nucl. Instr. and Meth. B* 2003 **B201** (1) 230.
- [7] Alexeev, V.L.; Fedorov, V.V.; Lapin, E.G.; Leushkin, E.K.; Rumiantsev, V.L.; Sumbaev, O.I.; Voronin, V.V. *Nucl. Instr. and Meth. A* 1989 **A284** 181; *Sov. Phys. JETP* 1989 **69** 1083.
- [8] Fedorov, V.V.; Voronin, V.V.; Lapin, E.G. Preprint LNPI-1644, Leningrad 1990 36p.; *J. Phys. G* 1992 **18** 1133.
- [9] Fedorov, V.V.; Voronin, V.V.; Lapin, E.G.; Sumbaev, O.I. Preprint PNPI-1944, Gatchina 1994 10p.; *Tech. Phys. Lett.* 1995 **21**(11) 881; *Physica B* 1997 **234–236** 8.
- [10] Forte, M. *J. Phys. G* 1983 **9** 745.
- [11] Shull, C.G.; Nathans, R. *Phys. Rev. Lett.* 1967 **19** 384.



- [12] Baryshevskii,V.G.; Cherepitsa,S.V. Phys. Stat. Sol. 1985 **b128** 379;  
Izvestiya Vuzov SSSR, ser. fiz. 1985 **8** 110 (in Russian).
- [13] Golub,R.; Pendlebury,G.M. Contemp. Phys. 1972 **13** 519.
- [14] Abov,Yu.G.; Gulko,A.D.; Krupchitsky,P.A. *Polarized Slow Neutrons*; Atomizdat;  
Moscow, 1966; 256p. (in russian).
- [15] Alexeev,V.L.; Voronin,V.V.; Lapin,E.G.; Leushkin,E.K.; Rumiantsev,V.L.; Fe-  
dorov,V.V. Preprint LNPI-1608, Leningrad 1990 12p.;  
Tech. Phys. Lett. 1995 **21**(11) 881.
- [16] Fedorov,V.V.; Voronin,V.V. in Physics of Atomic Nuclei and Elementary Particles,  
Proc. of the XXX PNPI Winter School; St.Petersburg, 1996; 123 (in russian).
- [17] Schuster,M.; Carlile,C.; Rauch,H. Z.Phys. 1991 **B85** 49;  
Jericha,E.; Carlile,C.; Rauch,H. Nucl. Inst. and Meth. 1996 **A379** 330.
- [18] Dombeck,T. ANL-report PHY-8624-HI-97;  
Dombeck,T.; Kaiser,H.; Koetke,D.; Peshkin,M.; Ringo,R. ANL-report PHY-9814-TH-  
2001;  
Dombeck,T.; Ringo,R.; Koetke,D.D.; Kaiser,H.; Schoen,K.; Werner,S.A.; Dombeck,D.  
Phys. Rev. A 2001 **64** 053607.
- [19] Forte,M.; Zeyen,C.M.E. Nucl. Instr. and Meth. A 1989 **A284** 147.
- [20] Voronin,V.V.; Fedorov,V.V.; Preprint PNPI-2293, Gatchina 1999 10p.
- [21] Baryshevsky,V.G. J.Phys. G 1997 **23** 509.
- [22] Hirsch,P.B.; Howie,A.; Nicholson,R.B.; et al., *Electron Microscopy of Thin Crystals*;  
Butterworths; London, 1965.
- [23] Fedorov,V.V.; Kir'yanov,K.E.; Smirnov,A.I. Sov. Phys. JETP 1973 **37** 737.
- [24] Rauch,H.; Petrachek,D. in Neutron diffraction; Ed. Duchs,H.; Dynamical neutron  
diffraction and its application; Springer, Berlin, 1978; 303.
- [25] Golub,R.; Lamoureux,K.L., Phys. Rep. 1994 **237** 1.
- [26] Voronin,V.V.; Fedorov,V.V.; Lapin,E.G.; Semenikhin,S.Yu. Physica B 2003 **335** (1-4)  
201-204.
- [27] Fedorov,V.V.; Lapin,E.G.; Semenikhin,S.Yu.; Voronin,V.V. Appl. Phys. A 2002  
**74**[Suppl.] s91-s93.
- [28] Voronin,V.V.; Lapin,E.G.; Semenikhin,S.Yu.; Fedorov,V.V. JETP Lett. 2000 **71**(2) 76.  
Preprint PNPI-2337; Gatchina 2000 12p.
- [29] Fedorov,V.V.; Voronin,V.V. Nucl. Instr. and Meth. B 2003 **201** 230-242.

- [30] Voronin,V.V.; Lapin,E.G.; Semenikhin,S.Yu.; Fedorov,V.V. Preprint PNPI-2376, Gatchina 2000 15p.; JETP Lett. 2000 **72**(6) 308.
- [31] Fedorov,V.V.; Lapin,E.G.; Lelievre-Berna,E.; Nesvizhevsky,V.; Petoukhov,A.; Semenikhin,S.Yu.; Soldner,T.; Tasset,F.; Voronin,V.V. Nuclear Inst. and Methods in Physics Research B 2005 **227** (1-2) 11-15.
- [32] Fedorov,V.V.; Lapin,E.G.; Semenikhin,S.Yu.; Voronin,V.V. Physica B 2001 **297**(1-4) 293.
- [33] Fedorov,V.V. in Proc. of XXVI Winter LNPI School; Leningrad, 1991; Vol.1, 65.
- [34] Fedorov,V.V.; Lapin,E.G.; Semenikhin,S.Yu.; Voronin,V.V. Appl. Phys. A 2002 **74**[Suppl.] s298-s301.
- [35] Voronin,V.V.; Lapin,E.G.; Semenikhin,S.Yu.; Fedorov,V.V. JETP Lett. 2001 **74**(5) 251-254.  
Preprint PNPI-2431; Gatchina 2001 14p.
- [36] Dress,W.B.; Miller,P.D.; Pendlebury,J.M.; Perrin,P.; Ramsey,N.F. Phys. Rev. D 1977 **15**(1) 9.